NASA/CR—2005-213999 AIAA–2001–3906

Search for Effects of an Electrostatic Potential on Clocks in the Frame of Reference of a Charged Particle

Harry I. Ringermacher
KRONOTRAN Enterprises, LLC, Delanson, New York

Mark S. Conradi
Washington University, St. Louis, Missouri

Brice N. Cassenti
United Technologies Research Center, East Hartford, Connecticut

November 2005

The NASA STI Program Office . . . in Profile

Since its founding, NASA has been dedicated to the advancement of aeronautics and space science. The NASA Scientific and Technical Information (STI) Program Office plays a key part in helping NASA maintain this important role.

The NASA STI Program Office is operated by Langley Research Center, the Lead Center for NASA's scientific and technical information. The NASA STI Program Office provides access to the NASA STI Database, the largest collection of aeronautical and space science STI in the world. The Program Office is also NASA's institutional mechanism for disseminating the results of its research and development activities. These results are published by NASA in the NASA STI Report Series, which includes the following report types:

- TECHNICAL PUBLICATION. Reports of completed research or a major significant phase of research that present the results of NASA programs and include extensive data or theoretical analysis. Includes compilations of significant scientific and technical data and information deemed to be of continuing reference value. NASA's counterpart of peer-reviewed formal professional papers but has less stringent limitations on manuscript length and extent of graphic presentations.

- TECHNICAL MEMORANDUM. Scientific and technical findings that are preliminary or of specialized interest, e.g., quick release reports, working papers, and bibliographies that contain minimal annotation. Does not contain extensive analysis.

- CONTRACTOR REPORT. Scientific and technical findings by NASA-sponsored contractors and grantees.

- CONFERENCE PUBLICATION. Collected papers from scientific and technical conferences, symposia, seminars, or other meetings sponsored or cosponsored by NASA.

- SPECIAL PUBLICATION. Scientific, technical, or historical information from NASA programs, projects, and missions, often concerned with subjects having substantial public interest.

- TECHNICAL TRANSLATION. English-language translations of foreign scientific and technical material pertinent to NASA's mission.

Specialized services that complement the STI Program Office's diverse offerings include creating custom thesauri, building customized databases, organizing and publishing research results . . . even providing videos.

For more information about the NASA STI Program Office, see the following:

- Access the NASA STI Program Home Page at ***http://www.sti.nasa.gov***

- E-mail your question via the Internet to help@sti.nasa.gov

- Fax your question to the NASA Access Help Desk at 301–621–0134

- Telephone the NASA Access Help Desk at 301–621–0390

- Write to:
  NASA Access Help Desk
  NASA Center for AeroSpace Information
  7121 Standard Drive
  Hanover, MD 21076

NASA/CR—2005-213999 AIAA–2001–3906

Search for Effects of an Electrostatic Potential on Clocks in the Frame of Reference of a Charged Particle

Harry I. Ringermacher
KRONOTRAN Enterprises, LLC, Delanson, New York

Mark S. Conradi
Washington University, St. Louis, Missouri

Brice N. Cassenti
United Technologies Research Center, East Hartford, Connecticut

Prepared for the
37th Joint Propulsion Conference and Exhibit
cosponsored by the AIAA, SAE, AIChE, and ASME
Salt Lake City, Utah, July 8–11, 2001

Prepared under Contract NAS3–00094

National Aeronautics and
Space Administration

Glenn Research Center

November 2005

Acknowledgments

Thank you to Marc Millis for having the daring and fortitude to envision and create the BPP program and support this effort as part of it. It is an honor to be included in the first trials. Caleb Browning, Mark Conradi's graduate student, assembled the probe and took the very thorough NMR measurements supporting the conclusions of this work. Mark Conradi led as well as participated in the Washington University effort and contributed the excellent and novel NMR probe designs permitting such precise measurements. Brice Cassenti expended considerable effort developing the classical and quantum theory supporting the work, the detail of which is largely relegated to the Appendices (half the report). We thank Judy Keating for her assistance in organizing the final report and providing insightful "clock suggestions." We also thank Larry Mead for supportive discussions revolving around this new view of General Relativity.

Available from

NASA Center for Aerospace Information
7121 Standard Drive
Hanover, MD 21076

National Technical Information Service
5285 Port Royal Road
Springfield, VA 22100

Available electronically at http://gltrs.grc.nasa.gov

Executive Summary

A series of Nuclear Magnetic Resonance (NMR) experiments were performed to search for a change in the precession rate of the proton magnetic moment in a hydrogen atom subjected to an intense electrostatic potential, as predicted by a new theory coupling space-time to matter and charge. The theory self-consistently imbeds classical electrodynamics within the framework of non-Riemannian space-time by way of introduction of an electrodynamic Torsion tensor into Einstein's equations. It predicts that an intense, external electrostatic potential should measurably shift the internal clock of a charged particle analogous to the gravitational red shift. The internal clock refers to time as seen by a particle of charge-to-mass ratio, e/m, in its rest frame.
The precession rate (Larmor frequency) of the proton was set to 354 MHz in an 8.4T magnetic field of a superconducting magnet. The three experiments included:

(1) A proton subject to a spatially and temporally constant 5kV electrostatic potential –voltage on versus voltage off and voltage reversed NMR signals.
(2) A proton subject to a spatially constant but time varying 6kV electrostatic potential.
(3) A proton in a hydrogen atom physically moved through a spatially non-uniform, constant 5kV electric field–voltage on versus voltage off and dummy voltage NMR signals

No change in the proton's clock (the 354 MHz proton NMR resonance in a hydrogen atom) was observed in any of the three experiments. The experiments were done very carefully so that shifts in frequency of as little as 0.01ppm - that is about 3 Hz out of 354 MHz – could be observed. 5,000V was typically used resulting in a predicted shift of approximately 5ppm, more than enough to see with the stated sensitivity. The null results of the first two experiments were consistent with the predictions of the new theory and thus were not definitive. The third experiment was particularly important. The null result could not be explained by the present theory. This theory is, like the theory of gravitation, a single particle theory. However, a hydrogen atom also has an electron that interacts with the proton. In order to maintain the single particle character of a metric theory while simultaneously including the effects of the electron, a new conjecture, the "Clock Principle" (CP) is proposed. This principle states that the work done on the proton's clock changes its time. This automatically includes the work done by all the forces acting on the proton, including the external electric field and the electron. The net work done on the proton by the external electric field is cancelled against the work done by electron's force on the proton. We take this to be the reason for no clock effect. This is not the usual picture envisioned by General Relativity (GR), a theory depending on geometry alone.

CP may be false for the present theory and only coincidentally true for GR due to the equivalence principle, leaving only potential rather than potential energy (and therefore work) responsible for time changes.

If CP is true, it follows directly that negative rest mass cannot exist. Its existence violates the equivalence principle. This does not preclude the existence of negative energy since the general energy-momentum relation has both positive and negative energy roots (see "Clock Conclusions").

If CP is shown to be false then it follows that no metric theory incorporating electromagnetism is possible, thus formally ending Einstein's dream through a real experiment.

We demonstrate CP for three clocks: the NMR clock, the atomic clock and the pendulum clock. These and all known clocks can be shown to satisfy the conjecture.

Table of Contents

I. Introduction

The goal of the present work is to investigate an electromagnetic alternative to exotic physics for the purpose of coupling matter to space-time. Electromagnetic forces have distinct advantages. They are 10^{40} times stronger than gravity. They can be manipulated at will. Resources to create intense fields of virtually any geometry are readily available. However, there is currently no accepted theory linking electrodynamics directly with the geometry of space-time other than to curve it via extremely high energy densities. The mainstream approach taken is "bottom up", attempting to unite all forces in the context of quantum gauge field theory which has to-date been successful in unifying the weak and electromagnetic forces and describing the strong force in what is known as "the standard model". Gravity and therefore space-time geometry remains isolated from the internal geometry of gauge theory.

The proposed experiment is a measurable, predicted consequence of a completed and solved theory [1], linking space-time geometry and electrodynamics, describing effects of intense electrostatic potentials on time as seen in charged particle reference frames. This is grounded upon E. Schrödinger's later works on gravitation theory [2]. In his work, Schrödinger attempted to link electromagnetism to geometry through a non-symmetric affine connection (Torsion tensor). He failed at the attempt, primarily because of an error of oversight. The theory upon which the present work is based corrects this error [3], resulting immediately in the definition of a new type of affine connection – an electrodynamic connection – that precisely matches Schrödinger's concepts and furthermore satisfies the classical equations of motion for both charge and spin, thus finding a common denominator for both external space-time coordinates and internal spin coordinates. Following Schrödinger, once the connection is identified, it is merely a formality to extract the Einstein field equations and find solutions subject to the appropriate boundary conditions for electromagnetic fields.

II. Theory and Approach

Ideal Experiment

The theory [summarized in Appendix A] predicts that a particle of charge e, and mass m, immersed in a suitable electric field but unshielded and supported will see, in its rest frame, a time differing from the proper time of an external observer arising from the electrostatic potential at its location. In general, from the theory, the time shift in a clock interval is related to the potential difference between the two points;

$$\frac{d\tau_2}{d\tau_1} = 1 + 2\kappa(\varphi_2 - \varphi_1) \tag{1}$$

where $\kappa = -e/mc^2$. As an example, let us suppose that we have a distribution of test charges, say free protons, between two concentric cylindrical electrodes, an inner cylinder of radius R_1 and an outer cylinder of radius R_2. We further suppose we are able to create a situation in which the protons are momentarily at rest while experiencing an intense electric field. For example, they may be at the extreme of an oscillation in a vacuum. The relation between proper time elements at any two positions r_1 and r_2 within the medium, for the case of a cylindrical potential was found as an exact solution of the theory and is given by

$$\frac{d\tau_2}{d\tau_1} = 1 + 2\kappa\Lambda \ln\frac{r_2}{r_1}\,, \tag{2}$$

where Λ is the line charge density. This equation is exactly analogous to that for the gravitational red shift. The negative electrode is the zero potential reference for the free proton.

One possible clock for such a test is Nuclear Magnetic Resonance. A proton placed in an intense electric field within a radio-frequency transverse field " H_1 " coil aligned orthogonally to a uniform magnetic field, H_0, is resonant at the Larmor frequency, $\omega = \gamma H_0$, where the gyromagnetic ratio, γ, for the proton spin is proportional to e/m. We thus have a natural clock. From eq.(2) we expect the proton's clock frequency to depend on its position with respect to the zero potential electrode at R_1:

$$\omega(r) = \omega(R_1)\left(1 + 2\kappa\Lambda \ln\frac{R_1}{r}\right) \tag{3}$$

The Larmor field distribution is then given by:

$$H(r) = H(R_1)\left(1 + 2\kappa\Lambda \ln\frac{R_1}{r}\right) \tag{4}$$

From this it is straightforward to calculate the NMR lineshape and shift that will result when the electric field is turned on as compared to the field off. This is accomplished by performing a convolution of eq.(4) with the sharp Lorentzian line (seen in Fig.1). Figure 1 shows the result of this calculation for $R_1 / R_2 = 0.50$. With the E-field off, all the protons resonate simultaneously at the Larmor frequency and a sharp sweep field line will result, it's width broadened by the H_0-field inhomogeneity and local fields. With the electric field on, protons at different potentials will contribute to the signal at different times in the sweep thus further broadening and shifting the line while reducing the line intensity. We assume the natural width is much less than the electrostatic broadening. Under ideal circumstances, for a supported proton in a 8T magnetic field with a 5kV/cm electric field, a line shift and broadening of approximately five parts per million is expected. Pulsed NMR with FFT evaluation can be used in place of line sweeps.

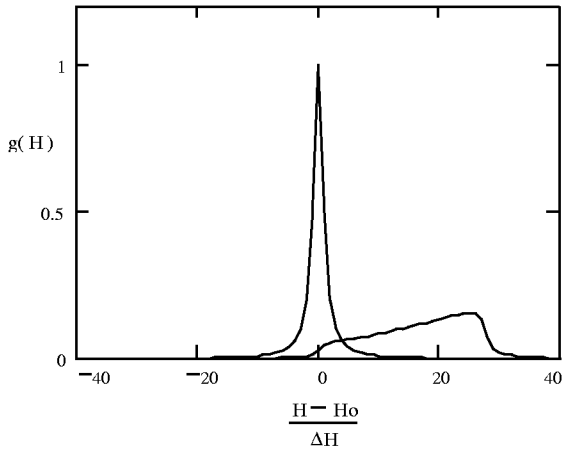

Figure 1. Normalized NMR lineshape as a function of magnetic field for electric field off (sharp line) and on (broadened). ΔH is the line width.

Present Approach

In practice it is experimentally difficult to "support" a charged particle. Generally, this can be accomplished electromagnetically, but then, by definition, the electric field and force at the particle location must vanish since the charge does not accelerate. Nonelectromagnetic support leaves only gravitational balance, which is very weak, and the nuclear force, which is very strong. At first sight, it would appear from the field equations that the presence of an electric field at the charged particle site is essential. But this may in fact not be the case, since the metric solutions to the theory depend on the potentials rather than on the electric fields. Thus it would appear that only potential differences are necessary to produce observable effects. The approach we have chosen uses the proton in a hydrogen atom. It is supported electromagnetically. The consequences of this approach will be the main subject of the conclusions of this work. A detailed description of the three experiments performed follows.

III. Experiments

Three experiments were performed. The first experiment, a constant potential applied to the proton in the hydrogen atom, was expected to produce null results both classically and within this theory. It was considered a "warm-up" experiment to verify the operating system. A constant potential is classically arbitrary to within a gradient of a scalar. This is a manifestation of the "Coulomb gauge condition" for the field and thus has no physical effects. Thus, a null result is expected.

The second experiment, a time-varying potential applied to the proton in the hydrogen atom, was initially expected to produce an effect. However, it was found during the course of this program that this theory was also invariant under a pure time-varying potential [4], a result consistent with the classical "Lorentz gauge condition" which is the relativistic generalization of the Coulomb gauge condition. That is, it states that the potential is also arbitrary to an additive time-derivative of a scalar. Thus, a null result is also expected.

The third experiment involves the physical displacement of a proton in a hydrogen atom through an electric field while NMR is performed on the proton. An observable shift in the proton NMR line is predicted. Care was taken to use a non-uniform electric field since Cassenti has shown [Appendix B] that a uniform field, such as that between two large, parallel, metal plates can lead to a possible null effect or, at the very least, confusion in interpretation of the data. Cassenti has calculated the electric field distribution for the chosen electrode geometry thus ensuring the non-uniformity of the field. In the present theory, in principle, only the potential difference between electrodes induces a frequency shift. The non-uniformity is merely "double insurance".

Experiment 1 – Constant potential

The 354 MHz, 8.4 Tesla rig was chosen for the experiments. This unit has a field homogeneity of 0.1 ppm or about 35 Hz, more than sufficient to resolve the predicted 5ppm effect. The proton sample was Benzene. The initial experiment, (Fig.2), was a simple free induction decay (FID) with the E-field on vs. off. The sample was enclosed in a 2mm thick aluminum can placed at high potential. Thus the E-field will vanish in the interior of the can at the sample but there will remain a constant potential. The voltage terminal (sample chamber) could be set + or – with respect to ground and the NMR FID was monitored.

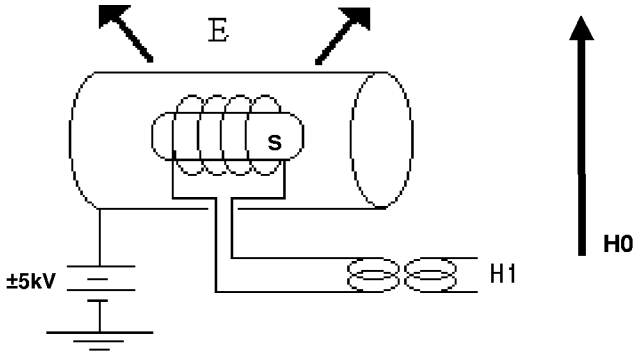

Figure 2. NMR "can" arrangement. External magnetic field, H0, is perpendicular to the radio frequency field, H1, applied through a coil wrapped around the proton sample, S. The 5kV electric field is applied outside the can leaving a constant 5kV potential inside.

An initial proton NMR line obtained from a water sample showed a field homogeneity of 0.3 ppm at a field intensity of 8.4 T. The goal was a homogeneity of 0.1 ppm or better. A field homogeneity of 10 ppb, far exceeding our goal and sufficient to resolve the smallest effects was achieved by shimming the magnetic field, reducing the sample size and confining the sample geometry to a long thin tube parallel to the external magnetic field thereby reducing end effects. Figure 3 shows the full double can probe with

inner can cover and outer ground shield removed. Figure 4 shows the probe head details before and after the sample geometry change. Figure 5 shows the probe head with the inner can in place and outer ground can removed.

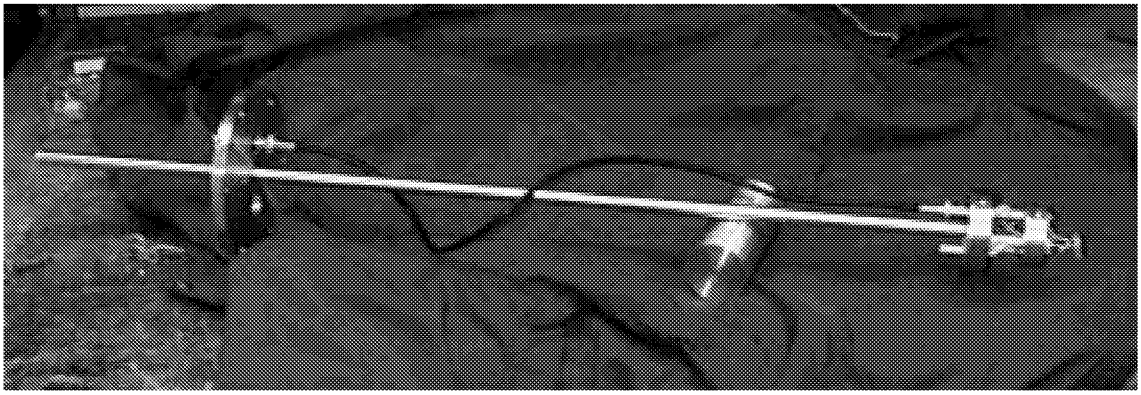

Figure 3. Full probe assembly with double cans removed showing probe head.

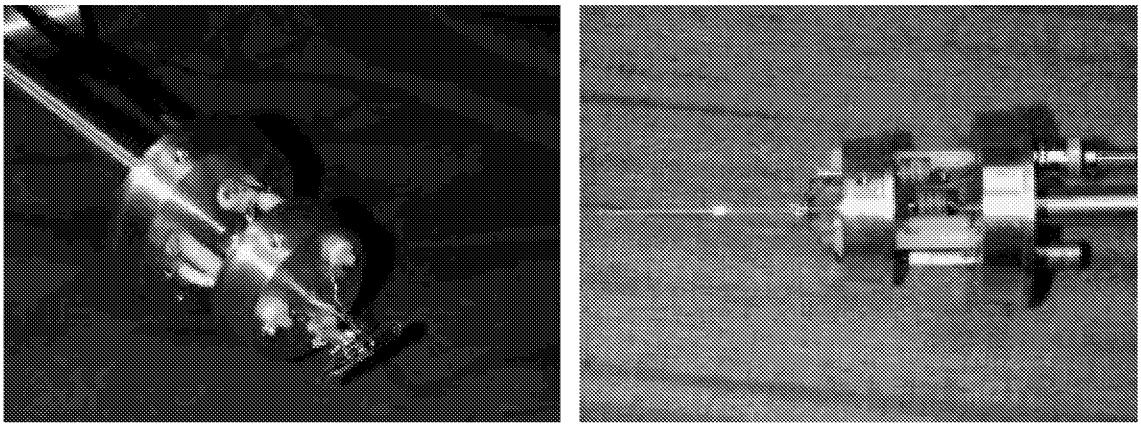

Figure 4. NMR probe head with low homogeneity sample geometry (left) and high homogeneity "needle" sample (right).

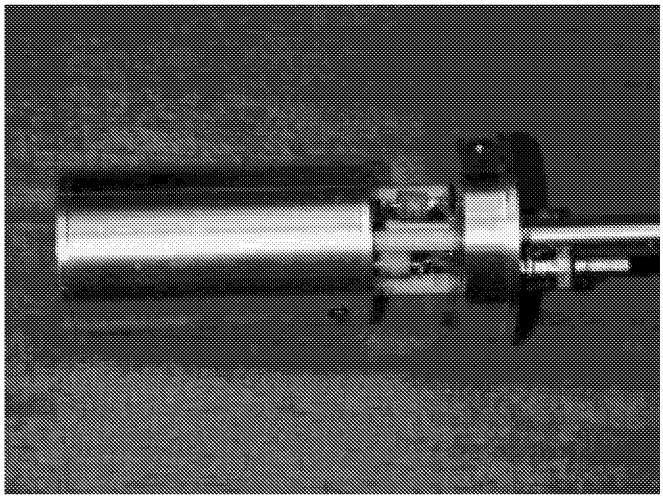

Figure 5. NMR probe head with constant potential inner can cover in place.

Following the high homogeneity tuning, the first trial of three major experiments was completed. A 5kV electric field was applied between the inner shielding can in which the proton sample (benzene) resided and the outer ground can. FID NMR was performed with field on and off in steady state. The electrostatic potential in the shield can was thus a constant 0 or 5kV. A second test was performed using a +3kV to –3kV potential reversal between the cans. In both tests the observed line shift, Figures 6a and 6b, was $\Delta\nu/\nu = 0 \pm 1.0\text{x}10^{-9}$, consistent with a null prediction of both classical E&M and the present theory.

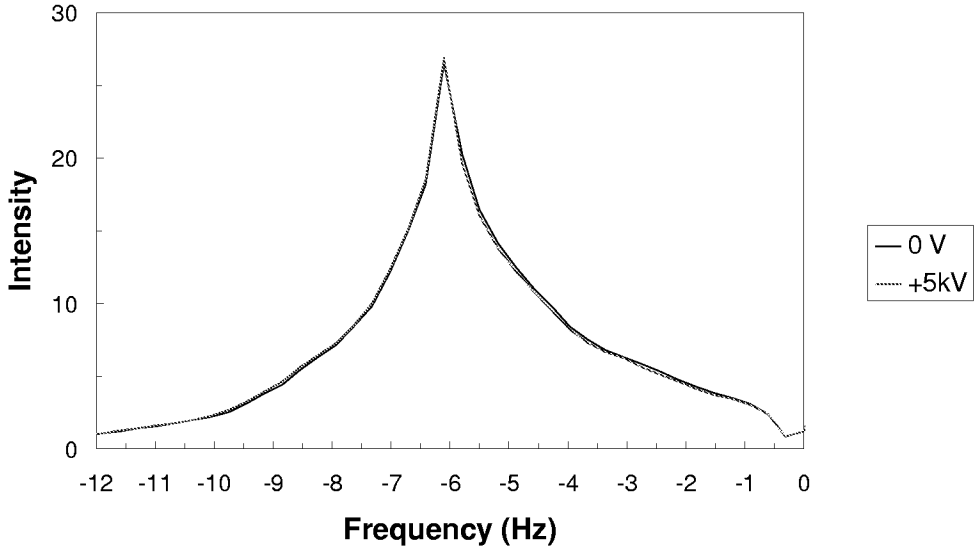

Figure 6a. NMR proton line in Benzene sample showing zero shift upon application of 5kV potential between shield can and ground can.

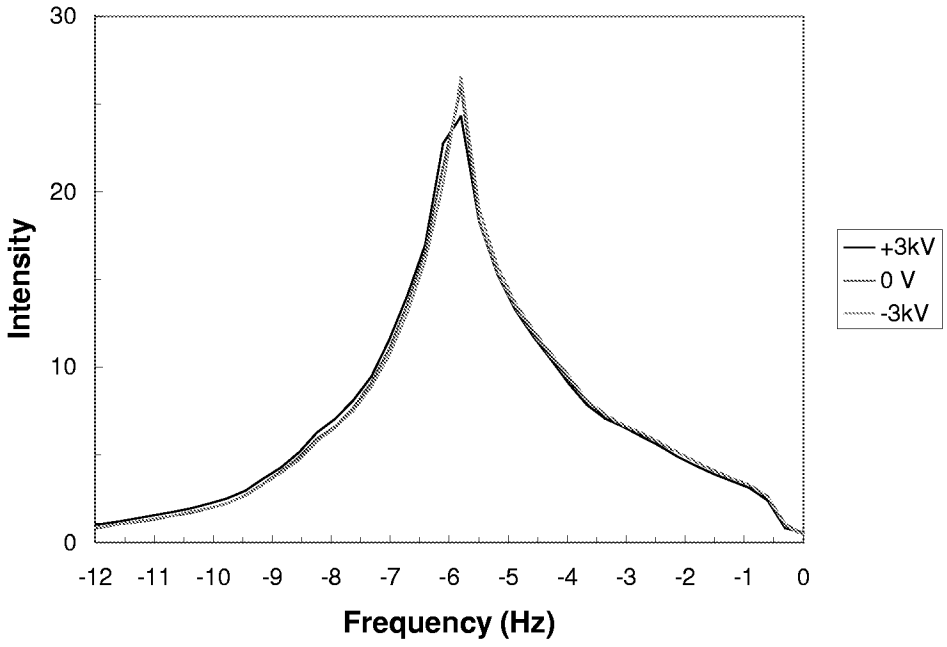

Figure 6b. NMR proton line in Benzene sample showing zero shift upon reversal of 3kV potential between shield can and ground can.

Experiment 2 - Time-varying potential

Originally, considerations in the theory suggested that a time-varying potential in the metric might be equivalent to a time-varying coordinate system and thus changes in clock rates. However subsequent calculation of this effect clearly showed that even the new Einstein equations were invariant under a time-varying potential in g_{00} .

The NMR "spin-echo" technique was employed in this experiment to monitor the precession. In the spin-echo technique, the proton's nuclear spins, precessing at 354 MHz and aligned along the external 8.4T magnetic field "z" direction, are first rotated 90° with respect to "z". This is accomplished by application of an rf pulse (90 pulse) at the Larmor frequency to a coil around the sample oriented in that direction. Following the rotation, the spin vectors dephase with characteristic time T2* and spread out in the "x-y" plane. At a time τ later a second rf pulse (180 pulse) is applied that rotates all the in-plane spin vectors an additional 180° which causes them to reverse directions in the x-y plane and thus rephase. The net rephased signal is the so-called "echo". Any miniscule line shifts occuring during the rephasing process will affect the echo amplitude and phase because an exact time reversal will not occur. Figure 7 shows the NMR spin-echo pulse sequence.

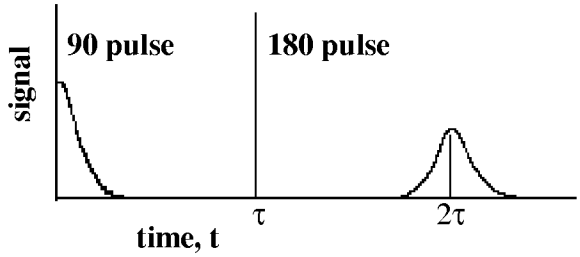

Figure 7. NMR spin-echo timing sequence showing spin rephasing time τ.

In order to ensure that the experiment had sufficient sensitivity, a small milliamp-level calibration current was injected into the NMR "shim coils" – those coils used to correct for small field gradients in the region of the sample in order to improve the magnetic field homogeneity. The current injection simulated the on-off and off-on step voltage procedure in order to quantify the expected NMR phase shift behavior. This calibrated response could then be compared to the observed step-voltage response as a function of τ. Figure 8 shows the NMR system response to the current injection. The "on-on" and "off-off" states refer to the current being constant – either on or off during the NMR acquisition period, τ, between the "90" pulse and the "180" pulse. These data overlap. There is no expected difference since these are steady states and the phase increases linearly with τ. This signal is the "control" data and represents the system response with no effects present. The rising "on-off" and falling "off-on" signals result from the current injection and are phase-reversed as expected. The phase difference between the control signal and the injected signal is 250° at τ =1 second, corresponding to 0.7Hz or 2ppb.

The proton sample (H_2O) was shielded inside an aluminum can as before. This ensures that the sample will see only a voltage potential, spatially constant inside the can, with zero electric field. The voltage on the can, with respect to ground, was changed during the NMR signal acquisition. The phase change, resulting from any magnetic line shifts arising from clock rate changes, was measured to an accuracy of approximately 2 degrees ($\Delta\phi = 0.035$ rad.) corresponding to a frequency shift of 0.005 Hz ($\Delta f_{min} = \Delta\phi / 2\pi T_{max}$; $T_{max} \cong$ T1=1 sec). This, in turn, corresponds to a frequency shift sensitivity of 0.005/354,000,000 or approximately 0.01ppb. . Upon application of a 5KV step-function (20 ms risetime) between the aluminum can and ground in both turn-on and turn-off modes, zero shift was observed in the NMR line to an accuracy of 0.01ppb.

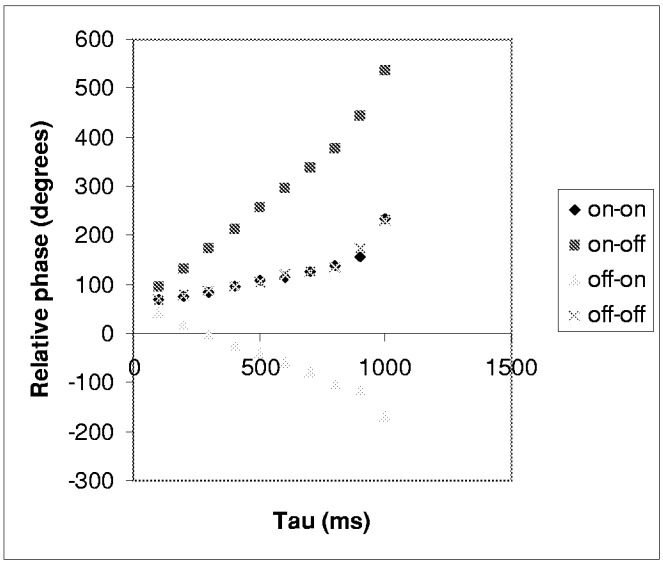

Figure 8. NMR calibration spin-echo phase signal as a function of 90-180 separation time Tau. Cycling refers to the switching of a small test magnetic field shift.

Figure 9 show the results of the second spin-echo experiment. For the control response, the "on-on" and "off-off" electric field states are reproduced. In the "on-off" state, the 5000V electric field is on and turned off at time τ. In the "off-on" state, the electric field is off and turned on at time τ. The risetime is approximately 30ms. τ was varied from zero to 1000 ms. No change from the control signal was observed to an accuracy of 0.01 ppb as evidenced by the same phase for the cases at each Tau.

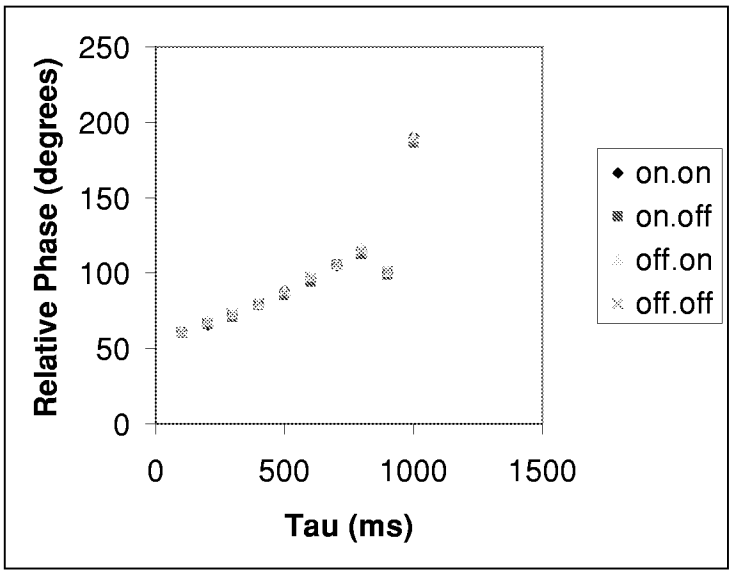

Figure 9. NMR data spin-echo phase signal as a function of 90-180 pulse separation time Tau. Cycling refers to the switching of the electric field.

Experiment 3 - Physical displacement of Hydrogen atom through high electric field

For the third and final experiment, hydrogen in benzene at room temperature was gravity-flowed between two electrodes, an upper one at ground potential and a lower one at +5000 V, both situated in the NMR coil in the external 8.4T magnetic field while NMR was performed with the electric field on and off. The electrodes were copper discs placed in the 3mm I.D. of glass tubing and connected to a high voltage source through glass/epoxy seals. The electrode spacing was 1.0 cm giving an average electric field of 5000V/cm. The 2-turn NMR coil diameter was 1.5 cm ensuring that the HV region was inside the coil. The coil was untuned to avoid radiation damping since the signal was already very large. The electrode spacing was chosen for two reasons: (1) to avoid the situation of "uniform electric field" which would have been approximately the case for spacings of 1-2mm or less. Cassenti has shown [Appendix B] that the case of uniform electric field for this theory is reducible to a Riemann-flat space, thus making interpretation of results more difficult or questionable. A non-uniform field, as in the present electrode geometry, ensures that this does not occur and that only the potential difference between electrodes – which is the same regardless of electric field – is relevant. (2) the larger spacing avoids electric breakdown effects , creating unwanted currents, in the benzene. Figure 10(a) shows the NMR coil system schematic. Figure 10(b) shows the actual assembly lying on its side and opened for inspection.

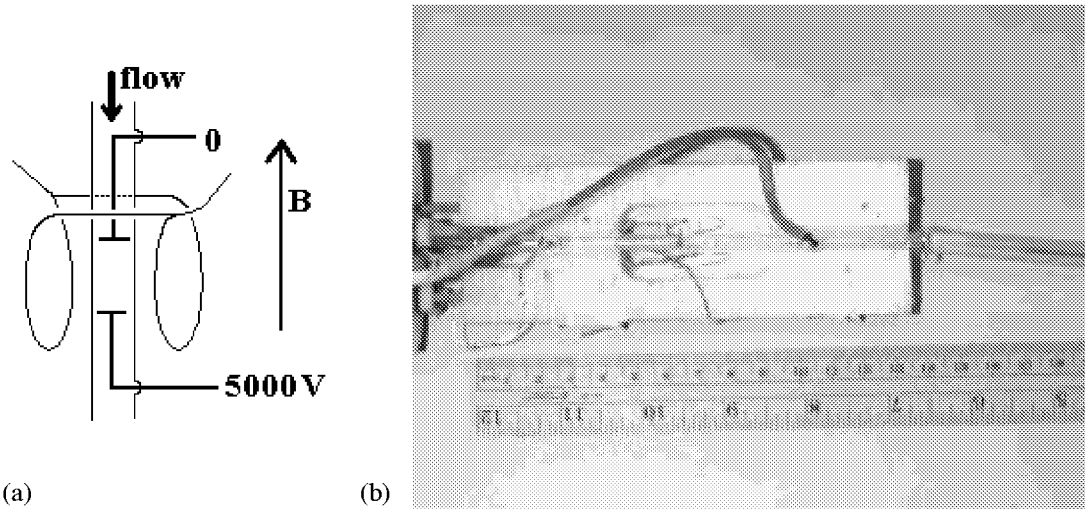

Figure 10. NMR coil and flow arrangement for E-field experiment: (a) schematic, (b) opened assembly on its side (flow left to right).

An NMR FID experiment was performed with and without flow. A 20-30 ms T_2 was obtained by careful adjustment of the B-field shim coils. The NMR line and effects of flow without the presence of an E-field were modeled. The T_2 value gives a line width of approximately 17 Hz ($\Delta f = 1/\pi T_2$). Figure 11(a) shows the measured NMR line as a function of flow velocity through the coil varying from 3 cm/s to 50 cm/s. Since the FID has a time constant of 20-30 ms, the proton must stay in the H1 field at least this long in order to contribute a significant time-shift signal arising from the maximum 5kV potential change. This corresponds to a flow speed of 15-30 cm/s, the mid-range of the chosen flows. Note that the measured shift with zero volts is approximately 10 Hz, from 0 to 50 cm/s flow rate, in approximate agreement with the theoretical calculation, Figure 11(b). Figure 12 shows the predicted lines for a maximum potential of 5000 Volts. The shift is at least ten times that for zero volts.

For the flow experiment, the NMR line was obtained for voltage off, voltage on, and a dummy voltage on (voltage on but HV cable disconnected). The probe voltage was discharged when the dummy experiment was performed. This data is shown in Figure 14a-14f. A typical NMR FID signal is shown in Figure 13 and compared to the calculated FID.

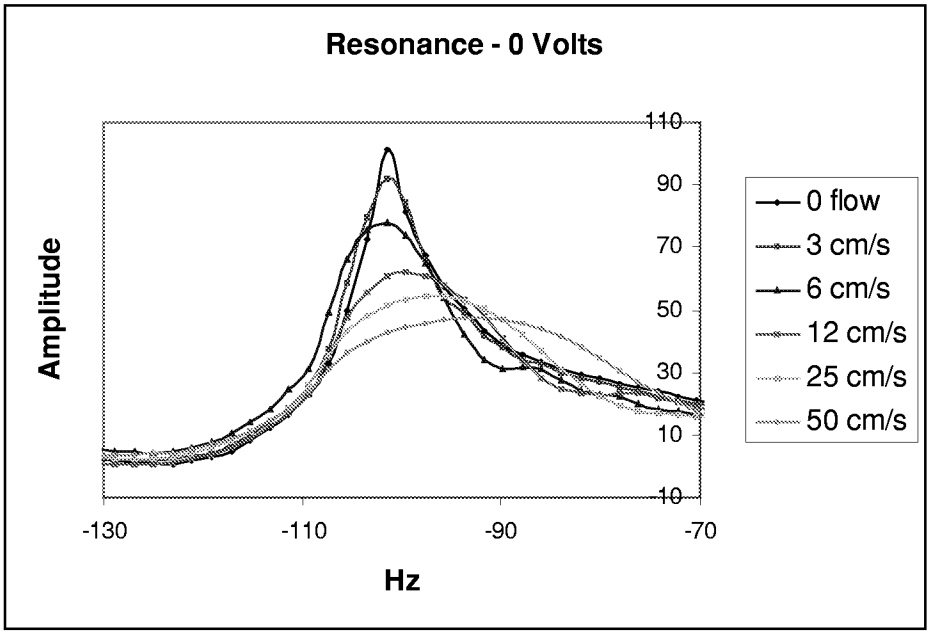

Figure 11(a). Measured NMR lines for zero E-field and flows from 0 – 50 cm/s.

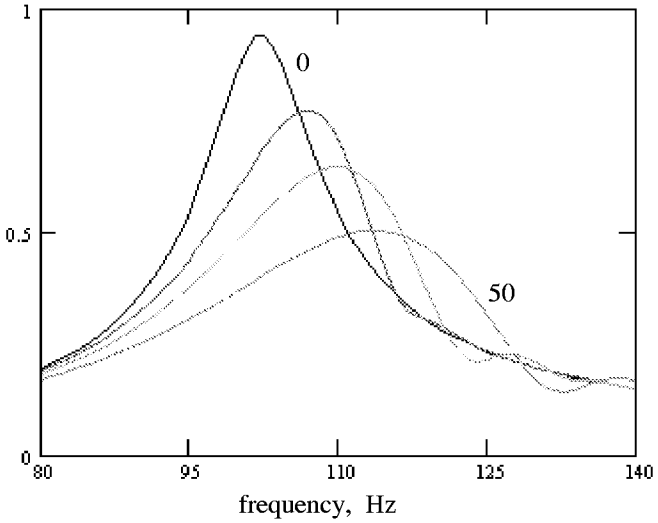

Figure 11(b). Calculated NMR lines for zero E-field for flows of 0, 12, 25 and 50 cm/s.

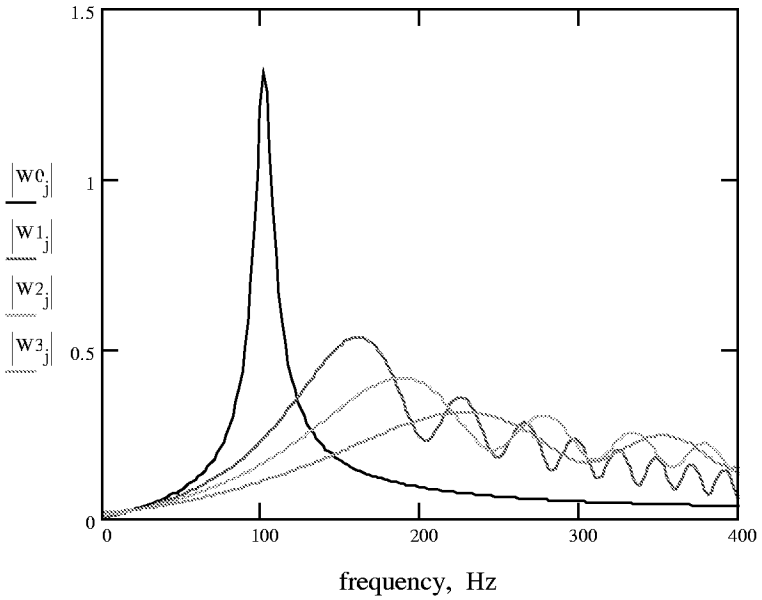

Figure 12. Calculated NMR lines for 5000V/cm E-field for flows of 0, 12, 25 and 50 cm/s.

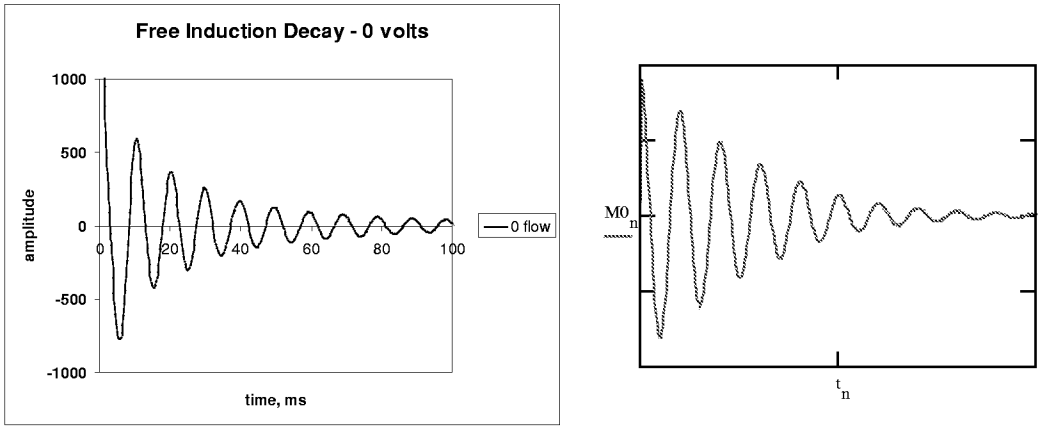

Figure 13. Typical measured FID signal (left) compared to calculated signal for prediction(right).

We note in Figure 14 that there is no change in the line position for each flow greater than the FFT resolution of ± 2 Hz corresponding approximately to a variation of 6 ppb, at least a hundred times smaller than the predicted shift of Figure 12. Figure 11 is the overlay of Figs. 14 for zero flow.

When the experiment was completed, the probe was disassembled and carefully inspected to ensure that all voltage connections were secure.

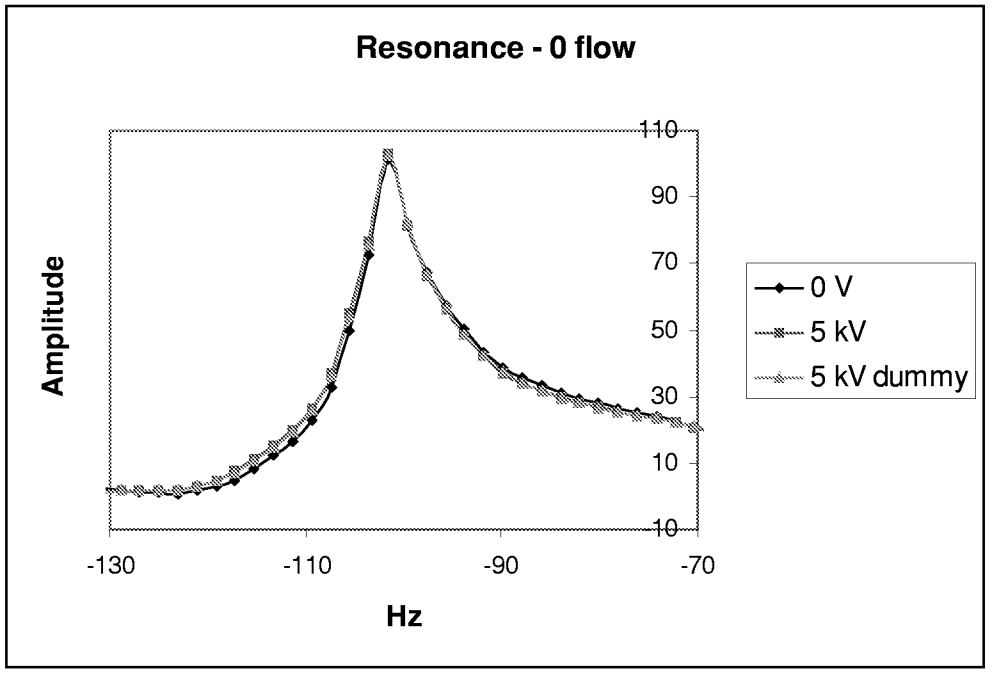

Figure 14a. Variation in NMR line for zero flow and applied voltage.

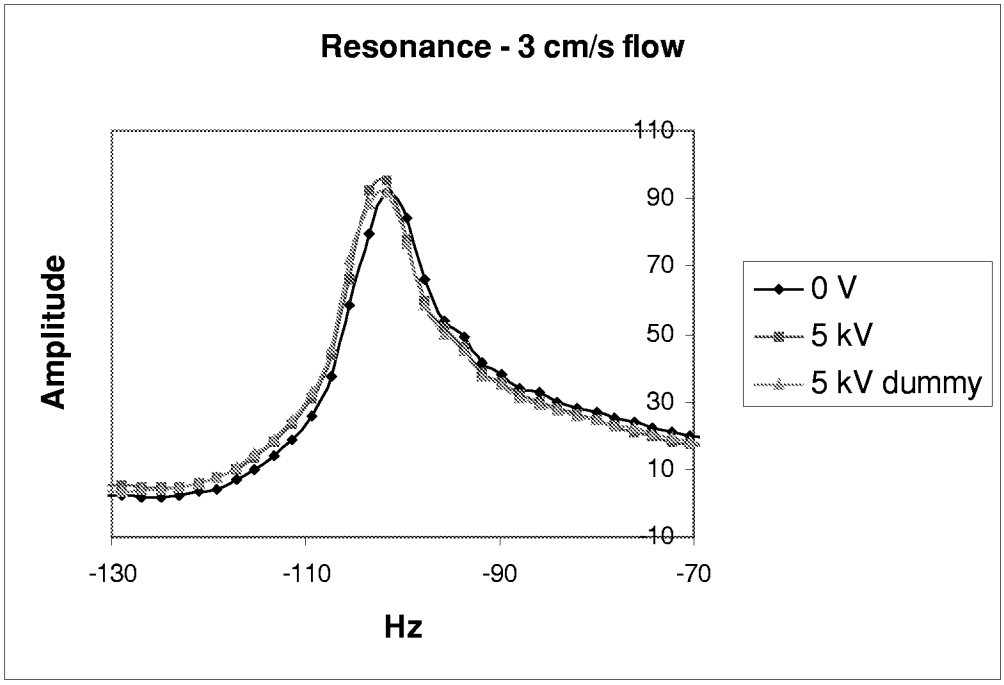

Figure 14b. Variation in NMR line at 3cm/s flow and applied voltage.

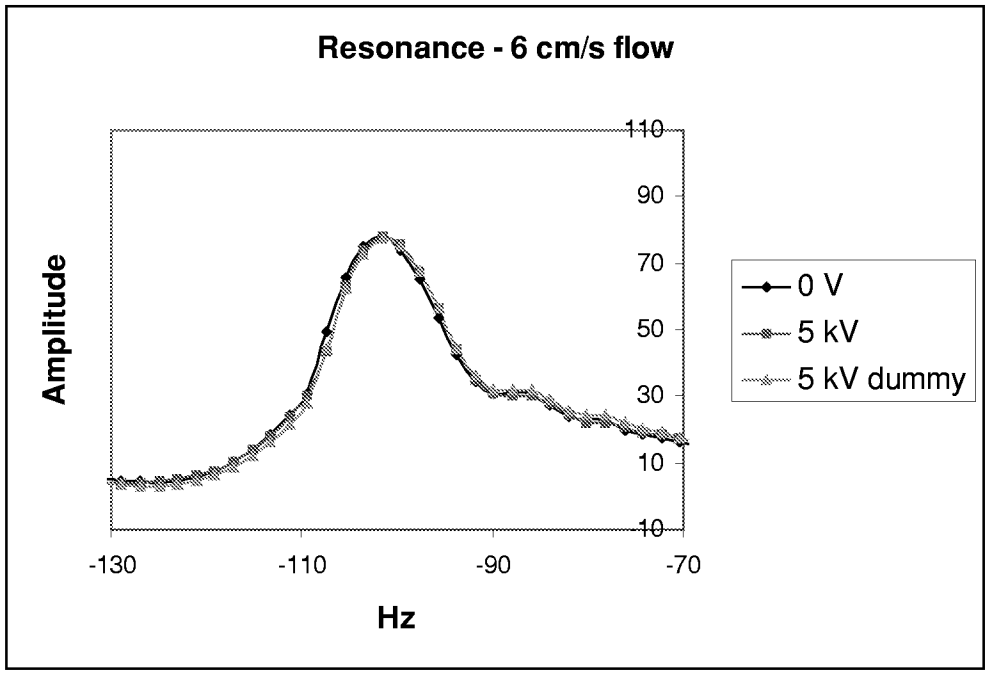

Figure 14c. Variation in NMR line at 6cm/s flow and applied voltage.

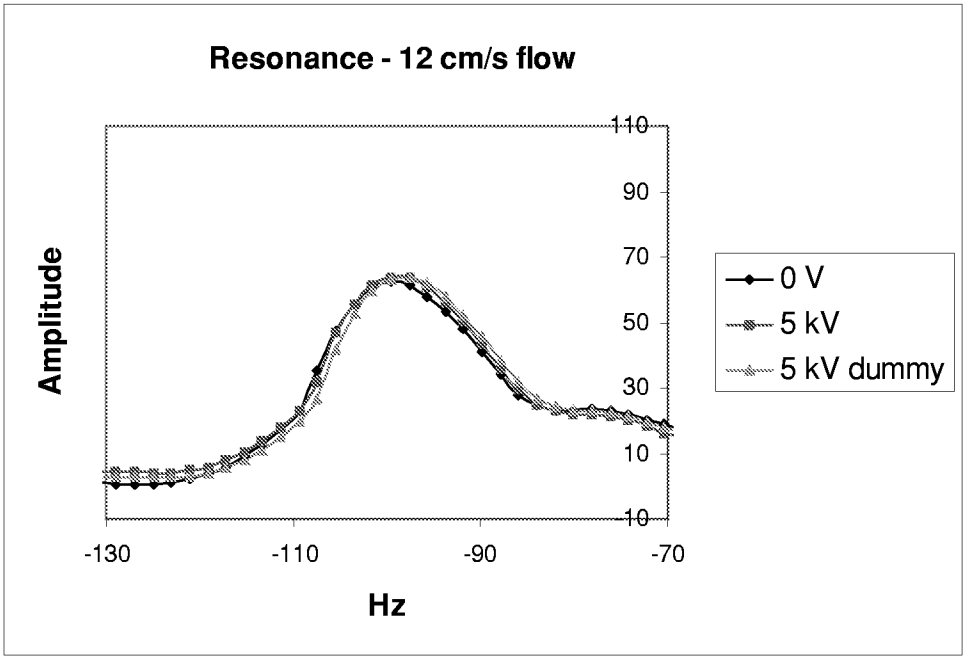

Figure 14d. Variation in NMR line at 12cm/s flow and applied voltage.

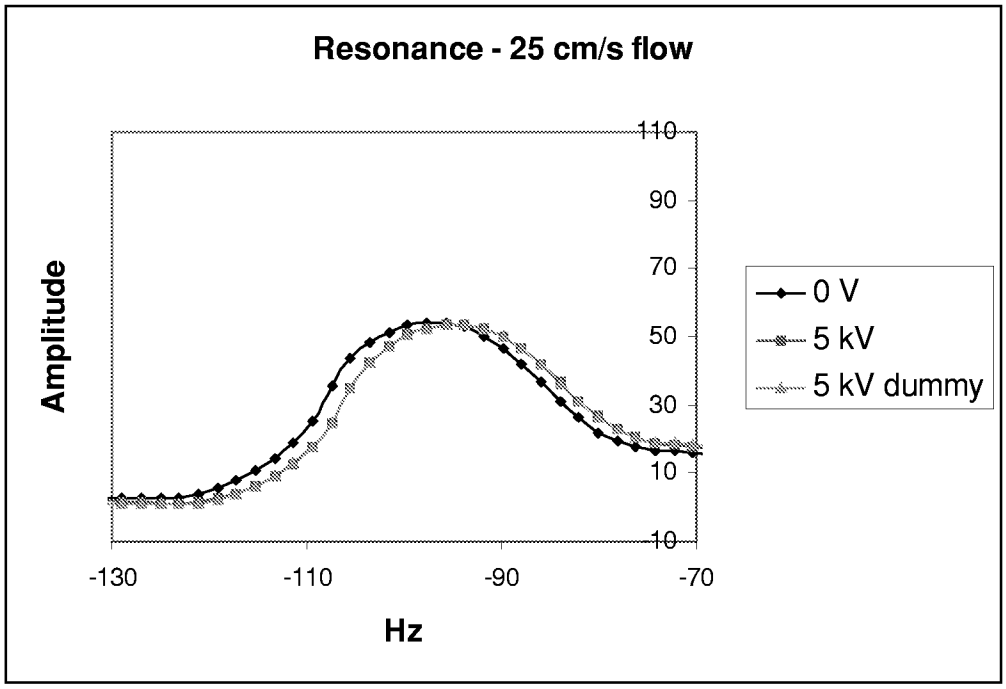

Figure 14e. Variation in NMR line at 25cm/s flow and applied voltage.

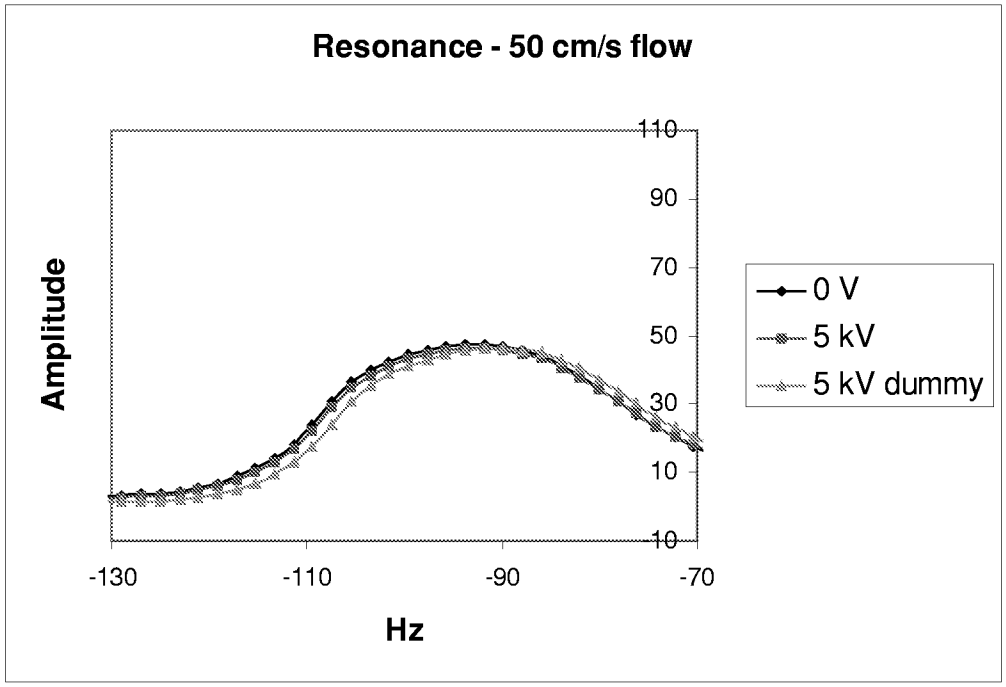

Figure 14f. Variation in NMR line at 50cm/s flow and applied voltage.

IV. Conclusions

Experimental Conclusions

All three experiments showed null results. The first experiment, constant potential applied to the proton in the hydrogen atom, produced a null result as expected and explained earlier. The second experiment, a time-varying potential applied to the proton in the hydrogen atom, also produced a null result as expected and explained. From the second experiment we have learned that the present theory is relativistically Gauge Invariant in the context of Maxwell's equations – as it should be.

The third experiment, physical displacement of a proton in a hydrogen atom through an electric field, was expected to produce a frequency shift in the NMR line. No change was observed to high precision. This is explained as follows. When a hydrogen atom is placed in an electric field, classically, only one effect is produced – an induced dipole moment of the atom resulting from the stretching of the electron orbital. Otherwise, no work is done on the hydrogen atom (except for the exceedingly small amount involved in stretching) since the work done on the proton is cancelled by the opposite work done on the electron(due to its negative charge) in the electric field. Furthermore, it is straightforward to show (Appendix C) that no work is actually done on the proton itself since the electric force on it is precisely balanced an opposing force, in the field direction, from the electron.

Implied Conclusions

The fact that no work is done on the proton provides a clue to explaining the present null result. The present theory is a single particle theory and does not take into account effects of other charged particles on the proton. It simply places the proton in a potential field and assumes there will be a metric effect similar to that in GR, which is also a single particle theory. It ignores the nearby electron as simply an additional non-interacting "test particle" in an external electric field. But that is wrong. The electron clearly interacts dynamically with the proton to cancel forces. Note the term forces.

The same can be stated for GR. If there is a nearby interacting massive particle, then GR will be inadequate in its present form to deal with this. This is a particularly glaring issue in GR since GR is independent of the mass of the test particle. GR will simply ask; what is the potential at the test particle location? If there is a nearby interacting particle in the same external field, GR will simply add the two potentials (one arising from the source and one from the second particle) at the location of the initial test particle to predict the effect on clocks. This, however, clearly ignores the dynamical effect of the second particle on the first. The metric, after all, can only accommodate one particle. That is the difficulty with the so-called "two body problem" in GR. The source of this difficulty seems to be the lack of a solid Hamiltonian formalism for GR that can accommodate forces.

A possible way out of this difficulty for both GR and the present theory is to use the concept of work done on the test particle by the external field and any other interacting particle. This approach still allows a single-particle metric theory, but accommodates the dynamics of a multiple-particle system as a cumulative effect on the single particle metric. Thus for the present theory, since zero work is done on the proton, there should be no dynamical effects and hence no clock change.

In the next section, we shall quantify this approach and show that it is consistent with GR in its present form, does not alter any known predictions of GR and can be generalized to include the present theory as well as predict new results within GR.

Relation of the Metric to the Lagrangian and Work Done

Let $\tilde{L}$ be defined as the specific Lagrangian or Lagrangian per unit rest energy,

$$\tilde{L} = \frac{(T - V)}{mc^2} \tag{5}$$

where T, V and m are the kinetic energy, potential energy and rest mass of the test particle respectively.

Suppose we are at rest at some height z in a gravitational field, so that $T=0$ and $V=mgz$, then $\tilde{L} = gz/c^2$. We have shown (Appendix E) for weak fields and nonrelativistic speeds that the proper time element can be written in terms of the Specific Lagrangian and coordinate time element as

$$d\tau = \sqrt{1-2\tilde{L}}\, dt. \tag{6}$$

Consider two positions in the gravitational field z_1 and $z_2 = z_1 + h$. Assume a proper time interval $d\tau_1$ at z_1 and $d\tau_2$ at z_2. Then, approximating the square root for weak fields,

$$\frac{d\tau_2}{d\tau_1} = 1 - \frac{g(z_2 - z_1)}{c^2} = 1 - \frac{gh}{c^2} \tag{7}$$

We can rewrite this in terms of the change in potential energy and Lagrangian:

$$\frac{d\tau_2}{d\tau_1} = 1 - \frac{mgh}{mc^2} = 1 - (\tilde{L}_2 - \tilde{L}_1) = 1 - \Delta\tilde{L} = 1 - \frac{(\Delta T - \Delta V)}{m_p c^2}\ . \tag{8}$$

In general, a variation in the Specific Lagrangian results in a change in the clock rate.

Referring more concisely to the metric for a single particle, p, we may express the Lagrangian change more clearly in terms of the net conservative work, W_c, done on p.

$$\Delta\tilde{L}_p = \frac{\Delta T_p + W_c}{m_p c^2} \tag{9}$$

The change in proper time intervals for the particle between two locations is thus

$$\frac{d\tau'}{d\tau} = 1 - \Delta\tilde{L}_p\,. \tag{10}$$

The weak-field, non-relativistic, metric for a given particle, i , acted upon by forces and hence net conservative work, W_{ci} ,done upon it by all other particles in the field is given by

$$d\tau_i^{\,2} = \left(1 - \frac{2W_{ci}}{mc^2}\right) c^2 dt_i^{\,2} - dx_i^{\,2} - dy_i^{\,2} - dz_i^{\,2}\ , \tag{11}$$

where

$$W_{ci} = \int \vec{F}_{ci} \cdot d\vec{r}_i\ . \tag{12}$$

We have rewritten the metric in this way because potential is not well-defined except through potential energy and work, where it is defined as work per unit mass in gravitation and work per unit charge in electromagnetism.

It can be shown that this formulation of GR does not alter the major known GR experiments, the perihelion shift of Mercury, the bending of light and the gravitational red shift to within the current experimental error. Indeed, the change to the perihelion shift very nearly removes the remaining 0.25% discrepancy. The measured precession of Mercury's perihelion is 43.11″ ± 0.21″/century [5]. GR predicts 42.98″. The present work corrects this to 43.18″/century, in closer agreement with the measurement.

Application to the hydrogen atom

The advantage of the work formulation is that it is true for any field. In particular, it is true for gravity as well as the present theory. There are now two possible interpretations for changes in clock rates. The first is that the potential enters directly through the metric and the second uses the work done on the

particle. Assume the first is correct, and consider the case of neutral monatomic hydrogen atoms moving at a constant speed through an electric field. The ratio of the clock rates, using equation (8), are given by (for weak fields and small velocities)

$$\frac{d\tau}{dt} = 1 - \frac{e\left[\varphi(z) - C\right]}{mc^2} + \frac{v_z^2}{2c^2} \quad , \tag{13}$$

where e is the electric charge of the proton, C is a constant, the potential energy is from an electric field that varies only with the z coordinate, and the velocity is constant and in the z-direction. If the clock rates are set to be the same at $z = z_0$ (i.e., $d\tau/dt=1$) then equation (13) becomes

$$\frac{d\tau}{dt} = 1 - \frac{e\left[\varphi(z) - \varphi(z_0)\right]}{mc^2}. \tag{14}$$

Note that the constant is given by

$$C = \varphi(z_0) - \frac{mv_z^2}{2e}. \tag{15}$$

For the nuclear magnetic resonance experiment we can take $dt = 1/f$ and $d\tau = 1/f_0$ where f_0 is now the rest frame frequency. Then

$$\frac{f}{f_0} = 1 - \frac{e\left[\varphi(z) - \varphi(z_0)\right]}{mc^2} \tag{16}$$

Thus, from a potential description only, we are left with an ill-defined consideration of the potential difference between two points affecting time and would conclude that the proton's clock should change. This approach clearly does not take into account the forces of the electron upon the proton. Hence we go to the next approach, consideration of forces and work done to define potential energy change for the proton.

An interpretation based on the work done requires a description of the forces acting on the proton. Consider the hydrogen atom oriented as in Figure 15. Here the electron is assumed to be a classical point particle. The electron and the proton orbit about a line through the common center of mass, with the centers displaced along the direction of the electric field.

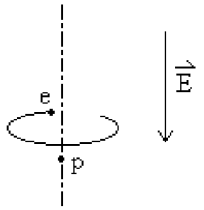

Figure 15. Hydrogen atom in an electric field

Note that there are two forces acting on either the proton or the electron. There is the internal attractive force acting on a line between the proton and the electron and the force due to the external electric field. The component of the internal force along the electric field exactly balances the force due to the external field. The remaining component of the internal force acts perpendicular to the motion for either the proton or the electron.

Hence, if the work interpretation is used no work is done on the proton and the frequency remains the same, resulting in the null experiment (see full discussion in Appendix E).

The Clock Principle

Potentials, potential energy and work

In the previous section we found a simple Lagrangian formulation that places gravitation on an equal footing with our theory in regards to changes in the temporal portion of the metric. This serves to simplify the interpretation of our results by a direct comparison to what is expected of standard gravitation theory under similar conditions. The Lagrangian formulation deals with kinetic and potential energy changes. Clocks raised in a gravitational field are at rest in the two positions and can be slowly moved between them. Thus the Lagrangian becomes simply the negative change of potential energy of the clock, moved from the lower position to the upper. But, for conservative fields, this is precisely the conservative work done on the clock. However, we must be careful and can no longer use the word "clock" loosely. When we refer to "clock" henceforth, we mean the *mechanism of the clock*. Thus we mean that work is performed on the *mechanism*. Clearly all clock mechanisms are driven by energy changes. What is not as obvious is that the mechanism of any clock must reflect the proper time variations in a gravitational field. For example, the mass-spring mechanism of a simple clock must somehow change with different heights in a gravitational field. Similarly, a pendulum clock must exhibit changes in its mechanism. Even an atomic clock is subject to this consideration. This brings us to the ***first clock postulate***:

1) ***Every clock has a mechanism which must be held accountable for observed changes in its measurement of time.***

We shall now examine the relationship between work and changes in clock time in a gravitational field. We use the notation "nc" to mean nonconservative and "c" for conservative. Conservative forces, by definition can be represented by a gradient of potential energy, V:

$$\vec{F}_c = -\vec{\nabla} V \tag{17}$$

Einstein Rocket -- Equivalence Principle for clock changes in a Gravitational Field

We shall employ the famous Einstein rocket "gedanken-experiment" to demonstrate our concepts. Consider a rocket lifting a mass, m, by a stiff wire in a gravitational field. Let us suppose that we adjust its thrust to precisely oppose the graviational pull on the mass. The rocket-mass system is now balanced and hovers, for example, at the surface of the earth. An arbitrarily small external force, $\vec{\varepsilon}$, may now raise the system to a height, h. This is shown in Figure 16. The force $\vec{\varepsilon}$ does no work on the system since it can be made arbitrarily small. However, upon rising a height h, due to the infinitesimal assistance of the guiding force, the rocket does work on the mass m. The potential energy of the mass is V_1 at the surface and V_2 at height h.

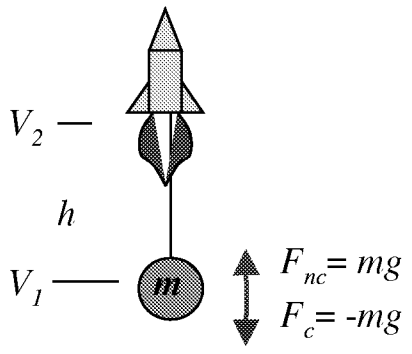

Figure 16. Balanced force configuration of a rocket-mass system

In this situation, the nonconservative force is that of the rocket. This is equal and opposite to gravity. We make the following definitions:

$$z_2 - z_1 = h \;\; ; \qquad d\vec{s} = dz\hat{k} \;\; ; \;\; \vec{g} = -g\hat{k} \tag{18}$$
$$\vec{F}_c = m\vec{g} \;\; ; \;\; \vec{F}_{nc} = -\vec{F}_c$$

Then the non-conservative work performed on the mass m by the rocket is

$$W_{nc} = \int_{z_1}^{z_2} \vec{F}_{nc} \cdot d\vec{s} = mgh\,. \tag{19}$$

and the conservative work performed on the mass m by gravity is

$$W_c = \int_{z_1}^{z_2} \vec{F}_c \cdot d\vec{s} = -mgh\,. \tag{20}$$

Now, from the definition of conservative work we have,

$$\Delta V = V_2 - V_1 = -W_c = mgh\,. \tag{21}$$

Summarizing, we find for the conservative work done on m:

$$W_c = -mgh = -\Delta V \tag{22}$$

Einstein rocket replaced by negative mass

Let us now reconsider the rocket of Figure 16. We can equally well replace the rocket by negative mass equal in magnitude to the lower positive mass - Fig.17. The earth's gravitational field repels negative matter and thus an amount $-m$ will precisely balance the force of attraction on m, a situation equivalent to the rocket. Note, however, that the inertial response of $-m$ to this is to fall downward along with m. Nevertheless, since only forces enter the definition of work, no work is done to maintain the position of the mass dipole and, indeed, just as in the case of the rocket, no work is done by an arbitrary small external force, $\vec{\varepsilon}$, that raises the rocket a height h in the gravitational field.

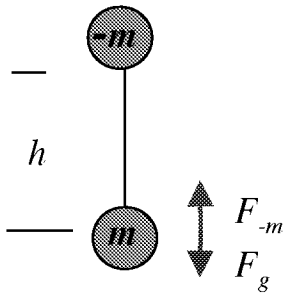

Figure 17. Balanced force configuration for rocket replaced by negative mass

We evaluate the work done in this situation. There are two forces acting on m, $\vec{F}_g$ and $\vec{F}_{-m}$. This time *both* forces are conservative. Therefore,

$$W_g = -\Delta V_g \qquad \text{and} \qquad W_{-m} = -\Delta V_{-m}\,. \tag{23}$$

The total work done on the mass m is zero because there is no change in the kinetic energy, since $\vec{F}_{-m} = -\vec{F}_g$.

$$W_{total} = \int \vec{F}_g \cdot d\vec{s} + \int \vec{F}_{-m} \cdot d\vec{s} = \Delta T = 0 \tag{24}$$

However, now the total work done on m is conservative since, unlike with the rocket, there are no non-conservative forces acting. The rigid wire transmits the conservative force from $-m$. Thus we find:

$$W_c = W_g + W_{-m} = 0 \tag{25}$$

This model of a massive neutral dipole is exactly equivalent to an electric neutral dipole such as the proton and electron of a hydrogen atom in an electric field. In the latter case, the two forces acting on the proton, the external electric field and the opposing force of the electron are both conservative. The total conservative work on the proton is zero when the atom is moved a distance h through a known potential difference [Appendix E]. That is precisely our experiment. There was no clock change observed.

This leads us to the ***second and third Clock Postulates***:

> ***2) External conservative work done on a clock mechanism is responsible for changes in its rate when the motion of the clock can be neglected.***
>
> ***3) When the clock is not at rest, the change in its rate arises more generally from the change in the Specific Lagrangian for the mechanism.***

The third postulate takes into account the change when there is kinetic energy present [Appendix E].

These postulates reconcile the observations and considerations of the present experiment with those observed for gravity. Therefore one should not expect to see a clock change in the imagined massive dipole experiment since there was no net conservative work done on m.

Inconsistency between General Relativity and existence of a neutral mass dipole

Now consider a clock on the mass *m* attached to the rocket. The mass m might itself be part of a clock mechanism. Upon reaching height *h*, the clock will change.
Assume a proper time interval $d\tau_1$ at z_1 and $d\tau_2$ at $z_2 = z_1 + h$. Then, we have shown that the relation between the two intervals is given by

$$\frac{d\tau_2}{d\tau_1} = 1 - \frac{gh}{c^2} = 1 - \frac{mgh}{mc^2} \tag{26}$$

and is related to the work, *-mgh* , done by gravity on *m*. But the mass *m* cannot distinguish between the pull of the rocket on the wire from that of the negative mass. In both instances the clock is displaced a height *h* and must change according to the single particle metric of GR. In the case of the negative mass , the Clock Principle states that since no net conservative work is done on m , no clock change will be observed.

Since we assume GR to be true, either the Clock Principle is false or a mass dipole cannot exist as the analogue of a charge dipole. Thus, if the clock principle is true, negative mass cannot exist.

If the clock principle is false, then work and energy change are not related in general to time change. It follows that a metric theory of forces other than gravitation cannot be constructed.

Clock Conclusions

We have arrived at the following three postulates regarding behavior of clocks and time:

1) Every clock has a mechanism that must be held accountable for observed changes in its measurement of time.

2) External conservative work done on the clock mechanism is responsible for changes in its rate when the motion of the clock can be neglected.

3) When the clock is not at rest, the change in its rate arises more generally from the change in the Specific Lagrangian, defined in terms of work, for the mechanism.

It is generally agreed that in order for a clock to indicate the passage of time, energy change in the mechanism is required. The mechanism itself is always reducible to a mass or energy. Thus, it appears that space is coupled to time through energy. When a clock is raised in a gravitational field, work is performed on the mechanism. Conservative work, W_c, performed on the mechanism changes its rate. W_c includes the net work done by all conservative forces acting on the mechanism. If W_c =0 so that applied forces opposing conservative forces are also conservative, then there will be no observed clock change. In general, a change in the specific Lagrangian $\tilde{L}$ will result in a change in the clock rate.

If conservative work changes clocks then ***negative mass cannot exist.*** . This does not preclude the existence of negative energy since the general energy-momentum relation has two roots,

$$E = \pm\sqrt{p^2c^2 + m^2c^4}$$

of which the positive root, in the rest frame of a particle of mass m ($p=0$), is the famous Einstein energy-mass relation.

V. Future Directions

The third experiment performed in this work leaves open the possibility that this theory and all metric theories of electromagnetism are invalid. One may inquire as to whether there is a definitive experiment, having learned from the present work, that would settle this issue. In fact we have identified two possible experiments – both involving free charges as opposed to the bound systems of the present work. These would provide unambiguous tests of the theory. Both test the Lagrangian formalism which is the generalization of the Clock Principle. These are; (1) an Electron Spin Resonance test of the Lagrangian formulation, and (2) a classical measurement of the quantum Aharonov-Bohm Effect. We will focus on an experimental description of (1) since (2) is considerably more exotic and exceedingly difficult.

(1) Microwave Cavity Test of the Single Particle Lagrangian Formulation

A conceptually simple, but technically difficult, test of the Lagrangian interpretation for a classical theory unifying gravity and electromagnetism would utilize a diode vacuum tube- consisting of two charged plates, at a constant potential, with electrons between the plates. The electrons accelerating from rest between the cathode to the anode would have a constant total energy (T+U=0) but the Lagrangian (T-U) would change by a factor of two in the metric. If Electron Spin resonance (ESR) measurements were performed on the electrons in the diode, then there would be a relative change in the resonant frequency of each electron as it moved from the cathode to the anode given by Eq.10, $d\tau'/d\tau = 1 + \Delta\tilde{L}_p = 1 + 2T/mc^2$. The result would be a broadening of the line by a factor of two over the shift due to the Lorentz time dilation – a readily distinguishable effect in the proper experiment.

Fairly large voltages (5kV or greater) would have to be used to produce an observable broadening. But large voltages will also result in large accelerations and short resident times for the electrons in the diode.

Hence it will be necessary to trap the electrons between the plates. This could be accomplished by alternating voltage between the plates at a sufficiently high frequency to prevent most electrons from reaching either plate. If the electrons are to be confined to within a centimeter, then the field strengths required for an observable shift in the ESR frequency will result in microwave frequencies. A microwave magnetron would be a more sensitive device in which to test these ideas. Advantage could be taken of the resonant cavity to excite the electrons but the measurement must still utilize ESR within the cavity so as to be performed in the electron rest frame as required by the theory.

(2) A classical measurement of the quantum Aharonov-Bohm Effect

In the Aharonov-Bohm Effect [9], an electron beam is split and impinges on a long, fine, solenoid, whereupon the two electron-wave components are permitted to interfere on a distant screen. This is all arranged in an electron microscope. A long solenoid is equivalent to a so-called "infinite solenoid". The internal field, B, is constant with flux Φ. Although the external field is zero, the vector potential is nonzero. Only magnetic fields generate observable forces – vector potentials are unobservable and do not-so there are no forces on the electron beam outside the solenoid. With the magnetic field off in the solenoid, the two interfering beams create an interference pattern consisting of bright and dark bands on the screen. With the field on, the pattern is observed to shift even though there are no forces acting on the beam. This effect is attributed to the quantum phase of the correlated beams which is directly affected by the vector potential. This is seen as a strictly quantum effect. However, we have shown (Appendix G) that the present theory exactly accounts for it through the Lagrangian approach. The expected effect is a small time delay of one beam relative to the other as they pass the solenoid. In order to convert this real time delay to a phase shift, to agree with QM, one must associate a frequency with the electron beam. That frequency is the so-called "zitterbewegung" frequency and is the natural frequency to choose.

Appendix A. On the Compatibility of Gravitation and Electrodynamics

The present work is a highly condensed summary of a theory that is shown to correctly represent both gravity and electromagnetism classically within a Pseudo-Riemannian geometry[1]. It is grounded upon a new affine connection which derives from an electrodynamic torsion acting upon charged particles in an electromagnetic field. The geometry is that seen by a charged particle and depends upon the electromagnetic potential at the particle location within a space-time that can include gravity. The present theory applies to weak fields and therefore does not couple the two fields. Present gravity experiments remain unaffected and the correct electromagnetic potentials derive from metrical solutions of the field equations. Thus both the Einstein equations and the Maxwell equations are satisfied by the metric solutions.

It is shown, however, that pure electromagnetic geometry should produce effects similar to those of gravity. These effects are resolved within the particle reference frame since that represents the simplest solution. The result is a consistent field theory with solutions and an experimental prediction.

In ref.[3] the new connection is derived from first principles but can be found effectively from introducing an electrodynamic torsion. The same connection was found by Schrödinger [2] but not identified or recognized as such - indeed he discarded the antisymmetic part of his connection(pure torsion) since it did not contribute to the motion.

This torsion, given by

$$\tilde{\Gamma}^{\lambda}_{[\mu\nu]} = \frac{\kappa}{2} u^{\lambda} F_{\mu\nu}, \tag{1}$$

does not alone contribute to the Lorentz motion of a charged particle. Its properly symmetrized contribution to the connection (eqn. 2 below) does, however. The pure torsion, eqn. (1) alone, was shown to be the source of the well-known Thomas Precession term in the "classical spin" equation of motion. It cannot be physically ignored. It can be said that the connection is fully determined by the metric tensor and the torsion as seen in eqn.(2). J. Vargas [6] has independently found the same torsion tensor from a Differential Forms approach.

The electrodynamic connection is:

$$\begin{aligned}
\tilde{\Gamma}^{\lambda}_{\mu\nu} &= \Gamma^{\lambda}_{\mu\nu} + \kappa\Lambda^{\lambda}_{\mu\nu} \\
\Gamma^{\lambda}_{\mu\nu} &= -\frac{1}{2} g^{\alpha\lambda}(\partial_{\mu} g_{\nu\alpha} + \partial_{\nu} g_{\mu\alpha} - \partial_{\alpha} g_{\nu\mu}) \\
\Lambda^{\lambda}_{\mu\nu} &= \frac{1}{2} g^{\alpha\lambda}(u_{\mu} F_{\nu\alpha} + u_{\nu} F_{\mu\alpha} - u_{\alpha} F_{\nu\mu}) \\
F_{\lambda\mu} &= A_{\mu;\lambda} - A_{\lambda;\mu}
\end{aligned} \tag{2}$$

u^{λ} is the test particle 4-velocity and $\kappa = -e/mc^2$.

Torsion is traditionally identified with angular momentum, which, it seems, has not borne physical fruit in the present context. The present work departs from tradition and clearly identifies it with electromagnetic objects.

In a second paper[3], the new Einstein tensor is developed from that connection. This follows the work of J. Schouten [7] exactly. The new Einstein tensor has both charged and "displacement" currents as sources. The electromagnetic energy density is ignored as contributing only higher order massive effects on the geometry in comparison to the new current terms. Solutions of the new field equations are presented that yield the classical electromagnetic potentials together with gravitational potentials in the appropriate cases. These solutions include (1) spherical electric plus gravitational field; (2) cylindrical line charge

field and (3), cylindrical uniform magnetic field.

Riemann and Einstein tensors with torsion:

The Riemann tensor is given by:

$$\tilde{R}^{\varepsilon}_{\mu\nu\sigma} = R^{\varepsilon}_{\mu\nu\sigma} + \kappa\frac{g^{\varepsilon\tau}}{2}(u_\nu F_{\mu\tau;\sigma} + u_\mu F_{\nu\tau;\sigma} + u_\tau F_{\mu\nu;\sigma} - u_\sigma F_{\mu\tau;\nu} - u_\mu F_{\sigma\tau;\nu} - u_\tau F_{\mu\sigma;\nu}) \tag{3}$$

This Riemann tensor satisfies the following Cyclic Identity upon alternating indices :

$$\tilde{R}^{\varepsilon}_{[\mu\nu\sigma]} = \kappa u^{\varepsilon}(F_{\mu\nu;\sigma} + F_{\nu\sigma;\mu} + F_{\sigma\mu;\nu}) \tag{4}$$

In deriving (3), covariant differentiation was passed through 4-velocities. Thus the identity (4) implicitly assumes this. Eqn. (4) can be derived from a Differential forms approach, as shown in the Addendum , without this assumption. The Einstein tensor is given by:

$$\tilde{G}_{\mu\nu} = G_{\mu\nu} + \frac{\kappa}{2}(u_\mu F^{\tau}_{\nu;\tau} + u_\nu F^{\tau}_{\mu;\tau} + u^\tau F_{\mu\nu;\tau} - 2u^\tau F_{\mu\tau;\nu} - 2g_{\mu\nu}u^\tau F^{\sigma}_{\tau;\sigma}) \tag{5}$$

The Einstein tensor separates into symmetric and antisymmetric parts(eq.6). The symmetric part provides the metrical field equation while its conservation yields the Maxwell source equations as our second field equation. The antisymmetric part yields the homogeneous Maxwell equations as a solution for arbitrary u since it must vanish. Eq. (4) also yields the homogeneous Maxwell equations.

$$\tilde{G}_{(\mu\nu)} = G_{\mu\nu} - \frac{\kappa}{2}u^\sigma(F_{\nu\sigma;\mu} + F_{\mu\nu;\sigma} - g_{\nu\sigma}F^{\tau}_{\mu;\tau} - g_{\mu\sigma}F^{\tau}_{\nu;\tau} + 2g_{\mu\nu}F^{\tau}_{\sigma;\tau}) \tag{6}$$

$$\tilde{G}_{[\mu\nu]} = \frac{\kappa}{2}u^\sigma(F_{\mu\nu;\sigma} + F_{\nu\sigma;\mu} + F_{\sigma\mu;\nu})$$

where real currents in (6) are defined from ,

$$F^{\cdot\tau}_{\mu;\tau} = -J_\mu$$

Following Schrödinger, the Einstein tensor on the right of eq.(6) is taken to vanish since this is purely gravitational and the electromagnetic field is assumed to contribute a negligible energy density compared to the massive source for this solution. This leaves G-tilda on the left with no apparent structure except as determined by its electromagnetic torsion effects on the right. Since we have shown that this tensor is symmetric and pseudo-Riemannian we assert that its structure will be that of the usual Einstein tensor but that it now is a more general function of a metric tensor that includes the effects of electromagnetic torsion. We can drop the tilda notation since g-tildas on the right will only contribute in second order. This leads us to the new Einstein equation.

Field equations and solutions:

The governing equations are chosen to be (for vanishing charge current sources):

$$G_{\mu\nu} = -\frac{\kappa}{2}u^\sigma(F_{\nu\sigma;\mu} + F_{\mu\sigma;\nu}) \tag{7}$$

$$F^{\mu\tau}_{\ \ ;\tau} = 0$$

$$F_{\mu\nu;\sigma} + F_{\nu\sigma;\mu} + F_{\sigma\mu;\nu} = 0$$

These equations are functions not only of the metric and electromagnetic fields but also of the test particle 4-velocity. The dependence on the 4-velocity is not unexpected since in classical correspondence the velocity-dependent Lorentz force must be accounted for and the connection describes precisely those

forces. This has been a bone of contention, but this is a classical theory and that is life. The test charge rest frame is chosen for simplicity in the solutions. Conservation of the Einstein tensor yields exactly the wave equation for the EM field and thus Maxwell's source equations:

$$G_{\mu\tau;}{}^{\tau} = -\frac{\kappa}{2} u^{\sigma} (F_{\mu\sigma;\tau;}{}^{\tau} + J_{\mu;\sigma} - J_{\sigma;\mu}) \tag{8}$$

This vanishes identically since it can be shown that the wave eq. is

$$F_{\mu\sigma;\tau;}{}^{\tau} = J_{\sigma;\mu} - J_{\mu;\sigma}$$

and thus the new Einstein tensor is conserved. Solutions of Eq.7 for the three cases described above are:

(1) Spherical Gravity plus Electric Field

The spherical interval is:

$$d\tau^2 = e^{\nu} dt^2 - e^{\lambda} dr^2 - r^2 d\theta^2 - r^2 \sin^2\theta d\phi^2 .$$

We ignore charge-mass (QM) product terms for our "zero coupling approximation" to find solutions:

$$e^{\nu} = 1 - \frac{2M}{r} - \frac{2\kappa Q}{r} ; \qquad e^{\lambda} = \left(1 - \frac{2M}{r}\right)^{-1} \tag{9}$$

$$E = \frac{Q}{r^2}$$

(2) Line Charge Electric Field

The cylindrical interval is given by:

$$d\tau^2 = e^{\nu} dt^2 - e^{\lambda} dr^2 - r^2 d\phi^2 - dz^2$$

The solutions are:

$$e^{\lambda} = 1 \tag{10}$$

$$e^{\nu} = e^{4\kappa\Lambda \ln(r/R)} \approx 1 + 4\kappa\Lambda \ln\left(\frac{r}{R}\right)$$

$$E = \frac{2\Lambda}{r}$$

We have taken $\kappa\Lambda << 1$. R is a constant of integration. Λ is the line charge density. The temporal metric coefficient fits the standard electric potential form, $1\text{-}2\kappa\Phi_{el}$, analogous to the gravitational form, $1+2\Phi_{gr}$ which was also the case for the spherical electric field solution. Φ_{el} is precisely the Maxwell line charge potential.

(3) Cylindrical Uniform Magnetic Field

For this case, the classic Rotating Frame metric was found to be an exact solution of the new Einstein equation . It can be stated that the magnetic field is equivalent to a rotating spatial frame. The interval is given by:

$$d\tau^2 = (1 - \omega^2 r^2) dt^2 - dr^2 - r^2 d\phi^2 - 2\omega r^2 d\phi dt - dz^2$$

The solutions are:

$$F_{01_{base}} = \omega Br \qquad (11)$$
$$g_{02} = \kappa Br^2$$
$$F_{01_{unit}} = (\vec{v} \times \vec{B})_r = \omega Br \;\; ; \quad F_{12_{unit}} = -B$$

$\omega = -\kappa cB$ is the cyclotron frequency for the orbit. EM field solutions are shown here with respect to standard unit vectors. B is a constant, the magnetic field. Note that the solutions are given with respect to standard "unit vectors". The solutions as found from the theory are with respect to "base vectors". The relation between unit and base vectors is given by:

$$F_{\mu\nu_{base}} = \sqrt{\left| g_{\mu\mu} g_{\nu\nu} \right|}\, F_{\mu\nu_{unit}} \quad \text{(not summed)}$$

Thus, for example, in the magnetic solution:

$$F_{12_{base}} = -Br \;\; ; \quad F_{01_{base}} = \omega Br$$

Mathematical issues

In order to obtain the above results, covariant derivatives were passed through the 4- velocities. The motivation for this, other than it greatly simplifies the work and gives physically correct results, is that the 4-velocity is a parallel vector field on the curve (geodesics) hence invariant to order κ in the field equations on the right. This was not a rigorous assumption at the time, just a compelling one. Below is a rigorous proof that 4-velocities effectively pass through covariant differentiation with respect to the coordinates in the Appendix using a Differential Forms approach [8]. The proof derives the fundamental Identity (eqn. 3) that Riemann satisfies and clearly shows that the four velocities fall out "as though they are constant". It therefore asserted in this work that differentiation can pass through the 4-velocities. A full rigorous approach might use a Finsler Space context (J. Vargas uses such an approach in his works) in which the 4-velocities are independent variables. But that is beyond the scope of the present work.

ADDENDUM: Validation of field equations using Differential Forms

The curvature 2-form for a differentiable manifold X_n referred to local coordinates x^ν endowed with a general nonsymmetric connection is given by:

$$\Omega^{\varepsilon}_{.\mu} = \frac{1}{2} R^{\varepsilon}_{.\mu\nu\sigma} dx^\nu \wedge dx^\sigma \qquad \text{(A1)}$$

The torsion 2-form is given by:

$$\Omega^{\varepsilon} = \frac{1}{2} S^{\varepsilon}_{.\nu\sigma} dx^\nu \wedge dx^\sigma \qquad \text{(A2)}$$

where,

$$\tilde{\Gamma}^{\varepsilon}_{[\mu\sigma]} = S^{\varepsilon}_{.\mu\sigma} = \frac{\kappa}{2} u^{\varepsilon} F_{\mu\sigma} \qquad \text{(A3)}$$

is the torsion tensor of this work. This torsion, although a direct product of a vector field on a curve in X_n with a tensor field on X_n is nevertheless valid with regard to defining a differentiable manifold since each field is itself differentiable on its domain. It can be shown that the exterior covariant derivative of the torsion 2-form is related to the curvature 2-form from the well known result [8]:

$$D\Omega^{\varepsilon} = -\Omega^{\varepsilon}_{.\lambda} \wedge dx^{\lambda} \tag{A4}$$

The crucial point of this result is that with differential forms, the covariant derivative is the absolute derivative, so that partial covariant derivatives, relevant in coordinate representations, need not be considered at all at this point.

Now the vector u^{ε} in general is the sum of a geodesic gravitational component and an electromagnetic contribution of order κ. We can ignore the electromagnetic contribution to the geometry since it will enter the field equations as order κ^2. Thus, since u^{ε} is then a vector on a geodesic, we may conclude without hesitation or question that

$$Du^{\varepsilon} = 0 \quad . \tag{A5}$$

We now expand (A4) using the above results to find:

$$DS^{\varepsilon}_{.\nu\sigma} \wedge dx^{\nu} \wedge dx^{\sigma} = \frac{1}{2} R^{\varepsilon}_{.\sigma\lambda\nu} dx^{\lambda} \wedge dx^{\nu} \wedge dx^{\sigma} \tag{A6}$$

Now utilizing the covariant partial on the spatial field F yields:

$$\kappa u^{\varepsilon} F_{\lambda\nu;\sigma} dx^{\lambda} \wedge dx^{\nu} \wedge dx^{\sigma} = R^{\varepsilon}_{.\sigma\lambda\nu} dx^{\lambda} \wedge dx^{\nu} \wedge dx^{\sigma} \tag{A7}$$

In component form this becomes precisely the equation, (4) above,

$$\kappa u^{\varepsilon} (F_{\lambda\nu;\sigma} + F_{\nu\sigma;\lambda} + F_{\sigma\lambda;\nu}) = \tilde{R}^{\varepsilon}_{\{\lambda\nu\sigma\}} \, . \tag{A8}$$

Thus Eq.(3) is a valid result and the fact that the partial covariant derivative passes through u^{ε} is an artifact of the component representation of a possible Differential Forms approach to this theory. I choose to adhere to the component approach and adopt the rule that *covariant partial differentiation with respect to local coordinates,* x^{ν}*, in* X_n *will pass through vector fields defined on a geodesic in* X_n.

Theory summary and conclusions:

We have shown that classical electrodynamics, neglecting radiative effects, can be embedded in a geometric framework in a self consistent way through the solutions of the field equations for the appropriate metrical and electromagnetic field variables. In the process, Maxwell's equations fall out naturally from conservation and symmetry requirements. From these solutions, not only are the correct electromagnetic fields found for a spherical electric field plus gravity, a line charge electric field and a uniform magnetic field, but also the expected electromagnetic potentials appear in the metric tensor alongside gravitational potentials. The procedure by which this is accomplished is partly grounded in Schrödinger's affine theory through a new "electrodynamic connection".

All that we have shown here is consistent with what is currently observed. Coexisting electric and gravitational fields act independently, within the scope of present measurements, on charged test particles, yet appear to share similar geometries. A classical neutral particle can pass with impunity through an electromagnetic field suggesting that electromagnetic fields do not influence the global geometry. In a sense we have a "relativity of geometry" since test charges with different κ experience correspondingly scaled geometries in their rest frames. Indeed, electromagnetic forces are velocity-dependent which stems from the nature of the Lorentz transformation.

Finally, it should be stressed that we have made several simplifications. We have only included order κ terms from the start. We have ignored the energy-momentum tensor. For the electric field solution we chose the rest frame and assumed spherical symmetry which is not strictly correct . We also ignored weak coupling terms.

Appendix B. Metric for Constant Fields

For constant electromagnetic fields (i.e., constant in space and time) a metric accurate to first order in the fields can be written as

$$g_{\mu\nu} = \eta_{\mu\nu} + \frac{e}{mc^2}\left(u_\mu F_{\nu\tau} + u_\nu F_{\mu\tau}\right)x^\tau . \tag{1}$$

Where $\eta_{\mu\nu}$ is the Lorentz metric in rectangular coordinates, $F_{\mu\nu}$ is a constant anti-symmetric tensor that will be identified with the electromagnetic fields, $u^\mu = dx^\mu/ds$ is the four velocity of the particle, x^σ are the coordinates (ct,x,y,z) and

$$ds^2 = g_{\mu\nu}dx^\mu dx^\nu . \tag{2}$$

Then to highest order in the fields

$$g^{\mu\nu} = \eta^{\mu\nu} - \frac{e}{mc^2}\left(u^\mu F^\nu{}_\tau + u^\nu F^\mu{}_\tau\right)x^\tau . \tag{3}$$

To first order in the fields the connections are

$$\Gamma^\sigma{}_{\mu\nu} = -\frac{e}{2mc^2}\eta^{\sigma\lambda}\left(u_\mu F_{\nu\lambda} + u_\nu F_{\mu\lambda}\right). \tag{4}$$

Note, to first order in the fields the Lorentz metric, $\eta_{\mu\nu}$, raises and lowers indices. Eq. (4) can be written as

$$\Gamma^\sigma{}_{\mu\nu} = -\frac{e}{2mc^2}\left(u_\mu F_\nu{}^\sigma + u_\nu F_\mu{}^\sigma\right). \tag{5}$$

The geodesics become

$$\frac{du^\sigma}{ds} = \frac{e}{mc^2}u^\nu F_\nu{}^\sigma \tag{6}$$

which are the correct equations of motion.

The rank four Riemann curvature tensor can now be calculated. The Riemann tensor contains both products of the connections and partial derivatives of the connections with respect to the coordinates. The products can be neglected since they are second order in the fields, and the derivatives vanish. Hence, the Riemann curvature vanishes and the space is Riemann flat (i.e., it is equivalent to a flat Lorentz space.)

Consider now the case of an electric field aligned along z. Then

$$F_{\mu\nu} = \begin{bmatrix} 0 & 0 & 0 & E \\ 0 & 0 & 0 & 0 \\ 0 & 0 & 0 & 0 \\ -E & 0 & 0 & 0 \end{bmatrix}. \tag{7}$$

For arbitrary four velocities the metric becomes

$$g_{\mu\nu} = \begin{bmatrix} 1+\frac{2eu_0Ez}{mc^2} & \frac{eu_1Ez}{mc^2} & \frac{eu_2Ez}{mc^2} & -\frac{e(u_0Ect-u_3Ez)}{mc^2} \\ \frac{eu_1Ez}{mc^2} & -1 & 0 & -\frac{eu_1Ez}{mc^2} \\ \frac{eu_2Ez}{mc^2} & 0 & -1 & -\frac{eu_2Ez}{mc^2} \\ -\frac{e(u_0Ect-u_3Ez)}{mc^2} & -\frac{eu_1Ez}{mc^2} & -\frac{eu_2Ez}{mc^2} & -1-\frac{2eu_3Ect}{mc^2} \end{bmatrix} \tag{8}$$

Note that the component

$$g_{00} = 1 + \frac{2eu_0 Ez}{mc^2} \tag{9}$$

is as expected.

The metric in equation (8) can be shown to be Riemann flat. Hence, the metric can be transformed to that of a freely falling (inertial) reference frame.

Consider the case of a particle starting at an arbitrary velocity. The components in the x and y directions can be made to vanish by rotating the coordinates so that $u_1=u_2=0$. The metric then becomes

$$g_{\mu\nu} = \begin{bmatrix} 1+\frac{2eu_0 Ez}{mc^2} & 0 & 0 & -\frac{e(u_0 Ect - u_3 Ez)}{mc^2} \\ 0 & -1 & 0 & 0 \\ 0 & 0 & -1 & 0 \\ -\frac{e(u_0 Ect - u_3 Ez)}{mc^2} & 0 & 0 & -1-\frac{2eu_3 Ect}{mc^2} \end{bmatrix}. \tag{9}$$

Performing a Lorentz transformation so that the velocity in the z direction vanishes(then $u_0=1$), the metric becomes

$$g_{\mu\nu} = \begin{bmatrix} 1+\frac{2eEz}{mc^2} & 0 & 0 & -\frac{eEct}{mc^2} \\ 0 & -1 & 0 & 0 \\ 0 & 0 & -1 & 0 \\ -\frac{eEct}{mc^2} & 0 & 0 & -1 \end{bmatrix}. \tag{10}$$

Equation (10) can be made diagonal by a change of coordinates. If we set

$$z = z' + \frac{eE(ct')^2}{2mc^2}. \tag{11}$$

while $t' = t$, $x' = x$, and $y' = y$ the new metric becomes

$$g'_{\mu\nu} = \begin{bmatrix} 1+\frac{2eEz'}{mc^2} & 0 & 0 & 0 \\ 0 & -1 & 0 & 0 \\ 0 & 0 & -1 & 0 \\ 0 & 0 & 0 & -1 \end{bmatrix}. \tag{12}$$

Appendix C. Potential Due to Two Oppositely Charged Circular Loops and Plates

Consider two charged loops with charge per unit length $\pm\sigma$ as shown in Figure 1. The loops have a radius, b, and are centered on the z-axis with a separation of L along z. The wires of each loop consist of a circular cross-section of radius a.

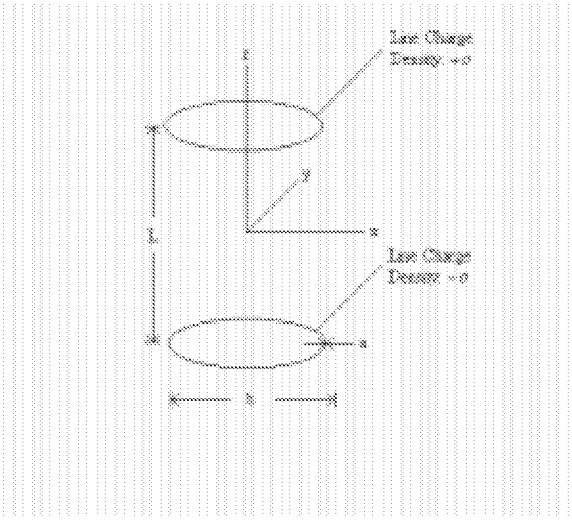

Fig. 1 Charged Loop Geometry

The centers of the loops are described by

$$x = b\cos\psi,\ y = b\sin\psi,\ z = \pm\frac{L}{2}. \tag{1}$$

The potential, φ, at all points is given by

$$\varphi = \frac{1}{4\pi\varepsilon_0}\int_0^{2\pi}\frac{\sigma b\,d\psi}{\sqrt{(x-b\cos\psi)^2+(y-b\sin\psi)^2+(z-L/2)^2}} - \frac{1}{4\pi\varepsilon_0}\int_0^{2\pi}\frac{\sigma b\,d\psi}{\sqrt{(x-b\cos\psi)^2+(y-b\sin\psi)^2+(z+L/2)^2}}. \tag{2}$$

Using polar coordinates, ($x = r\cos\theta$ and $y = r\sin\theta$) and letting $\phi' = (\pi - \psi + \theta)/2$, equation (2) becomes

$$\varphi = \frac{\sigma}{\pi\varepsilon_0}\int_0^{\pi/2}\frac{d\phi}{\sqrt{(1+\frac{r}{b})^2+(\frac{z-L/2}{b})^2-4\frac{r}{b}\sin^2\phi}} - \frac{\sigma}{\pi\varepsilon_0}\int_0^{\pi/2}\frac{d\phi}{\sqrt{(1+\frac{r}{b})^2+(\frac{z+L/2}{b})^2-4\frac{r}{b}\sin^2\phi}}. \tag{3}$$

The integrals in equation (3) are complete elliptic integrals of the first kind, *K(m)*, where

$$K(m) = \int_0^{\pi/2}\frac{d\phi}{\sqrt{1-m\sin^2\phi}}, \tag{4}$$

Equation (3) can now be written as

$$\varphi = \frac{\sigma}{\pi\varepsilon_0}\left(\frac{K(m_-)}{\rho_-} - \frac{K(m_+)}{\rho_+}\right), \tag{5}$$

where $\rho_\pm = \sqrt{(1+\frac{r}{b})^2 + (\frac{z \pm L/2}{b})^2}$, and $m_\pm = \frac{4(r/b)}{\rho_\pm^2}$.

Figures 2 and 3 illustrate the potential between the loops. The potentials are related to the charge density through

$$\frac{V_0}{2} = \frac{1}{2}\left[\varphi(r = b + a, z = L/2) + \varphi(r = b - a, z = L/2)\right] \tag{6}$$

Figure 2 demonstrates that the potential is fairly linear over the center forty percent of the axial distance between the loops and does not vary significantly over the radial coordinates. Figure 3 shows a variation of less than ten percent in the potential at the surface of the loops.

The solution between two charged wire loops can be readily extended to two finite disks by integrating over the radius of the loops. If the voltage is constant on the surface of the disks then a charge distribution that varies with the radius will be required. For the case of two disks of outer radius *b* and thickness *h* the potential is given by

$$\varphi = \frac{h}{\pi\varepsilon_0}\int_0^b \frac{\rho(r')K(m_-)r'dr'}{\sqrt{(r+r')^2 + (z - L/2)^2}} - \frac{h}{\pi\varepsilon_0}\int_0^b \frac{\rho(r')K(m_+)r'dr'}{\sqrt{(r+r')^2 + (z + L/2)^2}} \tag{7}$$

For a charge distribution given by

$$\rho(r') = \rho_0 \ , \tag{8}$$

the constant ρ_0 can be set to obtain the correct voltage on the plates. Figure 4 shows the variation in the potential between the plates for the apparatus at Washington University.

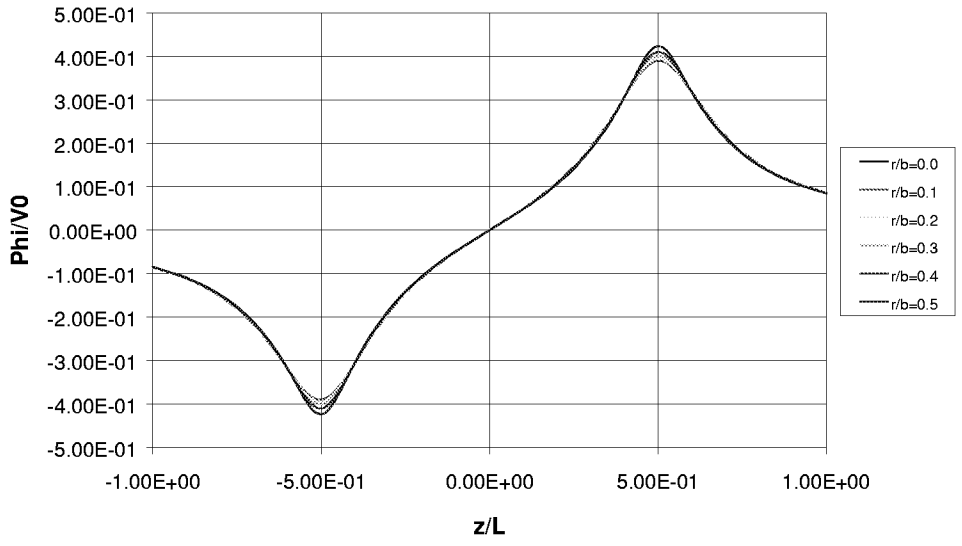

Fig. 2 Potential Between Two Wire Loops for a=0.25mm, b=1.5mm, L=10mm

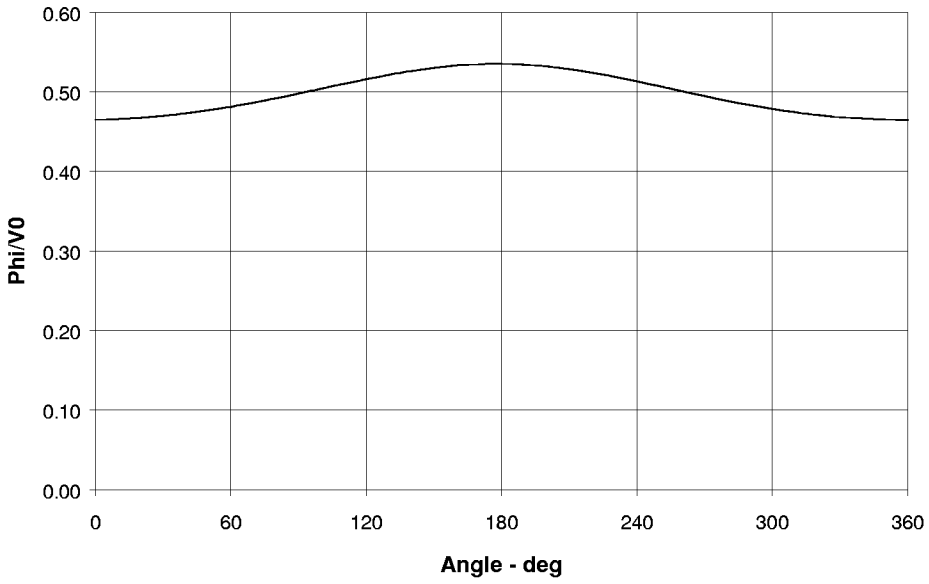

Fig. 3 Potential at Loop Surface for a=0.25mm, b=1.5mm, L=10mm

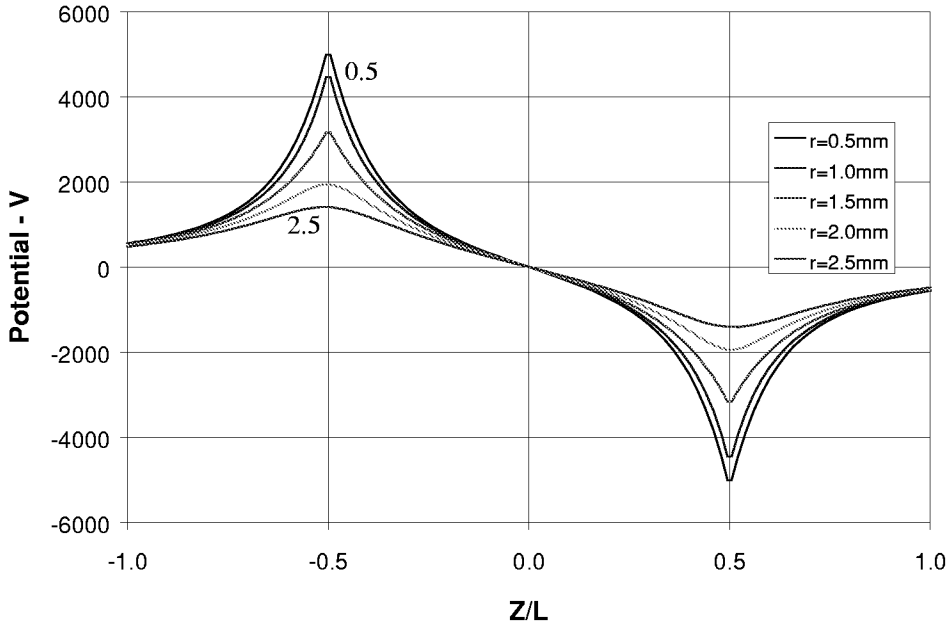

Fig. 4 Potential for Disks, b=1.5mm, L=10.mm

Appendix D. Potential for Hydrogen in Electric Fields

For a single hydrogen atom in an electric field, $\vec{F}$, the energy, E_T, is

$$\frac{1}{2}m_e v_e^2 + \frac{1}{2}m_p v_p^2 + \frac{q_p q_e}{4\pi\varepsilon_0 \left|\vec{r}_p - \vec{r}_e\right|} + q_p \vec{r}_p \cdot \vec{F} + q_e \vec{r}_e \cdot \vec{F} = E_T \,. \tag{1}$$

q_p is the charge on the proton (+e), q_e is charge on the electron (-e), m_p and m_e are the masses of the proton and electron respectively, v_p and v_e are the speeds of the proton and electron respectively, and $\vec{r}_p$, and $\vec{r}_e$ are the position vectors of the proton and the electron respectively. In rectangular coordinates the position vectors can be written as

$$\vec{r}_p = x_p \vec{i} + y_p \vec{j} + z_p \vec{k} \ , \tag{2}$$

and

$$\vec{r}_e = x_e \vec{i} + y_e \vec{j} + z_e \vec{k} \quad . \tag{3}$$

Changing the velocities to momentum and substituting for the charges, equation (1) becomes

$$\frac{p_e^2}{2m_e} + \frac{p_p^2}{2m_p} - \frac{e^2}{4\pi\varepsilon_0 r} + e\vec{F} \cdot \left(\vec{r}_p - \vec{r}_e\right) = E_T \,. \tag{4}$$

Where

$$r = \sqrt{(x_p - x_e)^2 + (y_p - y_e)^2 + (z_p - z_e)^2} \,. \tag{5}$$

For a field in the z direction ($\vec{F} = F\vec{k}$), the wave equation, from equation (4), becomes

$$-\frac{\hbar^2}{2m_e}\nabla_e^2\Phi - \frac{\hbar^2}{2m_p}\nabla_p^2\Phi - \frac{e^2\Phi}{4\pi\varepsilon_0 r} + eF(z_p - z_e)\Phi = i\hbar\frac{\partial\Phi}{\partial t} \,. \tag{6}$$

Where Φ is the wave function,

$$\nabla_e^2 = \frac{\partial^2}{\partial x_e^2} + \frac{\partial^2}{\partial y_e^2} + \frac{\partial^2}{\partial z_e^2} \,, \tag{7}$$

and

$$\nabla_p^2 = \frac{\partial^2}{\partial x_p^2} + \frac{\partial^2}{\partial y_p^2} + \frac{\partial^2}{\partial z_p^2} \,. \tag{8}$$

Converting to center-of-mass position, $\vec{R}$, and relative position, $\vec{r}$ coordinates, where

$$(m_p + m_e)\vec{R} = m_p \vec{r}_p + m_e \vec{r}_e \,, \tag{9}$$

and

$$\vec{r} = \vec{r}_e - \vec{r}_p \,. \tag{10}$$

Then

$$\vec{r}_p = \vec{R} - \frac{m_e}{m_p + m_e}\vec{r} \,, \tag{11}$$

and

$$\vec{r}_e = \vec{R} + \frac{m_p}{m_p + m_e}\vec{r}\,. \tag{12}$$

The wave equation (6) now becomes

$$\frac{\hbar^2}{2M}\overline{\nabla}^2\Phi + \frac{\hbar^2}{2\mu}\nabla^2\Phi + \frac{e^2\Phi}{4\pi\varepsilon_0 r} - eFz\Phi = -i\hbar\frac{\partial\Phi}{\partial t}. \tag{13}$$

Where

$$M = m_p + m_e\,, \tag{14}$$

$$\mu = \frac{m_p m_e}{M}\,, \tag{15}$$

$$\overline{\nabla}^2 = \frac{\partial^2}{\partial X^2} + \frac{\partial^2}{\partial Y^2} + \frac{\partial^2}{\partial Z^2}\,, \tag{16}$$

and

$$\nabla^2 = \frac{\partial^2}{\partial x^2} + \frac{\partial^2}{\partial y^2} + \frac{\partial^2}{\partial z^2}\,. \tag{17}$$

For the steady response we can use separation of variables, where

$$\Phi(X,Y,Z,x,y,z,t) = \Psi(X,Y,Z)\psi(x,y,z)e^{i(\overline{E}+E)t/\hbar}\,. \tag{18}$$

$$\frac{\hbar^2}{2M\Psi}\overline{\nabla}^2\Psi + \frac{\hbar^2}{2\mu\psi}\nabla^2\psi + \frac{e^2}{4\pi\varepsilon_0 r} - eFz = \overline{E} + E\,. \tag{19}$$

We can take

$$\frac{\hbar^2}{2M}\overline{\nabla}^2\Psi = \overline{E}\Psi\,. \tag{20}$$

Then

$$\frac{\hbar^2}{2\mu\psi}\nabla^2\psi + \frac{e^2\psi}{4\pi\varepsilon_0 r} - eFz\psi = E\psi \tag{21}$$

Classically the potential energy at the electron's position, V_e is

$$V_e = -\frac{e^2}{4\pi\varepsilon_0 r} - \frac{m_p}{M}eFz - eFZ\,, \tag{22}$$

and at the proton's, V_p, is

$$V_p = -\frac{e^2}{4\pi\varepsilon_0 r} - \frac{m_e}{M}eFz + eFZ\,. \tag{23}$$

Note that the total potential energy is the sum of the last two terms in each equation (22) and (23) plus one-half the sum of the first terms in equations (22) and (23). That is the total potential energy is the

sum of the potential energies due to the external forces plus one-half the sum of the internal forces, since the internal forces can only be counted once. We should also note that the total energy for the electron and the proton must include the kinetic energy of each.

The potential, φ, appearing in the metric in g_{00} is

$$\varphi = \frac{V}{mc^2}. \tag{24}$$

The potential for the electron or the proton can be found by substituting V_e or V_p for V in equation (24) respectively. The wave function can now be used to find the expected values for the potential of the electron and the proton using respectively,

$$\langle \varphi_e \rangle = \int_{\vec{R}} \int_{\vec{r}} \overline{\Psi}\, \overline{\psi} \varphi_e \psi \Psi d\vec{r}^{\,3} d\vec{R}^{\,3}, \tag{25}$$

and

$$\langle \varphi_p \rangle = \int_{\vec{R}} \int_{\vec{r}} \overline{\Psi}\, \overline{\psi} \varphi_p \psi \Psi d\vec{r}^{\,3} d\vec{R}^{\,3}. \tag{26}$$

Where $\overline{u}$ is the complex conjugate of u, and the wave functions have been normalized using

$$\int_{\vec{R}} \overline{\Psi}\Psi d\vec{R}^{\,3} = 1, \tag{27}$$

and

$$\int_{\vec{r}} \overline{\psi}\psi d\vec{r}^{\,3} = 1. \tag{28}$$

From equations (24) through (27), the expected potentials for the electron and the proton become

$$\langle \varphi_e \rangle = -\frac{e^2}{4\pi\varepsilon_0 m_e c^2} \int_{\vec{r}} \overline{\psi} \frac{1}{r} \psi d\vec{r}^{\,3} - \frac{m_p eF}{M m_e c^2} \int_{\vec{r}} \overline{\psi} z \psi d\vec{r}^{\,3} - \frac{eF}{m_e c^2} \int_{\vec{R}} \overline{\Psi} Z \Psi d\vec{R}^{\,3} \tag{29}$$

and

$$\langle \varphi_p \rangle = -\frac{e^2}{4\pi\varepsilon_0 m_p c^2} \int_{\vec{r}} \overline{\psi} \frac{1}{r} \psi d\vec{r}^{\,3} - \frac{m_e eF}{M m_p c^2} \int_{\vec{r}} \overline{\psi} z \psi d\vec{r}^{\,3} + \frac{eF}{m_p c^2} \int_{\vec{R}} \overline{\Psi} Z \Psi d\vec{R}^{\,3}. \tag{30}$$

The first two terms in equation (29) are in the energy for the Stark effect. The first two terms in equation (30) are at least m_e/m_p times smaller. The change in energy for the Stark effect in Hydrogen is (given in many texts) as

$$\Delta E_{Stark} = \frac{9}{4} a_0^3 F^2, \tag{31}$$

where a_0 is the Bohr radius. For a field of 10keV/cm, the change in energy for the electron is $0.82\text{x}10^{-6}$ $m_e c^2$ and for the proton is $0.45\text{x}10^{-9}$ $m_p c^2$. The last term in equations (29) and (30) represents the change in the potential due to the motion of the center-of-mass of the hydrogen atom. This can occur due the forced or free convection (i.e., flow) of the hydrogen or just due to the random motion of the atoms.

Consider the case of random motion of the atoms. The mean free path of the atoms at 300K, 10^5Pa, and using a cross-section of $2\text{x}10^{-10}$ m is about $3.4\text{x}10^{-7}$ m. Then the collision frequency is about 0.14 ns and in 1 μs there will be about 7100 collisions. The total distance traveled during the 1 μs is $3\text{x}10^{-5}$ m. Hence, the potential change in the metric for the proton (φ_p) is $3\text{x}10^{-8}$. For the electron, the potential change in the metric (φ_e) is $6\text{x}10^{-5}$.

Appendix E. Relation Between Metric, Lagrangian and Work on a Clock

We have seen that a possible explanation for our null result is that clock changes arise from work done on the system. In this case the system is a proton in a hydrogen atom. In order to permit an interpretation of the data it is necessary to relate the concept of mechanical work to the single particle metric of GR. We shall see that this approach will enable us to generalize this concept to any physical forces, in particular, the electromagnetic forces in the present theory. Below, we derive the relationship between the work done on a particle and it's space-time metric.

The Schwarzchild metric in rectangular coordinates, for weak fields and small velocities (i.e., $[d(ct)]^2 >> dx^2 + dy^2 + dz^2$), is

$$ds^2 = \left(1 + \frac{2\phi}{c^2}\right)c^2dt^2 - dx^2 - dy^2 - dz^2 . \tag{1a}$$

We may relate the gravitational potential, ϕ,to the potential energy of the test particle, V, by simply rewriting this equation, recalling that inertial and gravitational mass are equivalent:

$$ds^2 = \left(1 + \frac{2V}{mc^2}\right)c^2dt^2 - dx^2 - dy^2 - dz^2 , \tag{1b}$$

where

$$V = m\phi = -\frac{GMm}{r} \tag{2}$$

and m is the particle mass, c is the speed of light, G is the gravitational constant, M is the mass of the central body and r is the distance from the central mass.

The equations of motion for the metric above can be found by minimizing the action, I,

$$I = \int_{\tau_A}^{\tau_B} mcds \tag{3}$$

where $ds = cd\tau$. Substituting equation (1) into equation (3)

$$I = \int_{\tau_A}^{\tau_B} mc^2 \sqrt{\left(1 + \frac{2V}{mc^2}\right)\left(\frac{dt}{d\tau}\right)^2 - \frac{1}{c^2}\left[\left(\frac{dx}{d\tau}\right)^2 + \left(\frac{dy}{d\tau}\right)^2 + \left(\frac{dz}{d\tau}\right)^2\right]}\, d\tau = \int_{\tau_A}^{\tau_B} Ld\tau . \tag{4}$$

L is the Lagrangian function for the particle.
The conjugate energy, E, and momentum, $\vec{p}$, are given by

$$E = \frac{\partial L}{\partial\left(\frac{dt}{d\tau}\right)} = mc^2\left(1 + \frac{2V}{mc^2}\right)\frac{dt}{d\tau} \quad \text{and} \quad \vec{p} = \frac{\partial L}{\partial\left(\frac{d\vec{r}}{d\tau}\right)} = m\frac{d\vec{r}}{d\tau} \tag{5a,b}$$

The metric can now be used to write a relationship between the energy and the momentum with the aid of the expressions in equations (5):

$$m^2c^4 = \frac{1}{1 + \frac{2V}{mc^2}}E^2 - p^2c^2 \tag{6}$$

Solving for the energy and taking the positive square root yields

$$E = mc^2\sqrt{1+\frac{2V}{mc^2}+\left(1+\frac{2V}{mc^2}\right)p^2c^2}\ . \tag{7}$$

For weak fields and small velocities equation (7) becomes

$$E = mc^2 + V + \frac{p^2}{2m}\quad , \tag{8}$$

which is the correct nonrelativistic expression for the total energy.

Minimizing the action will result in equations of motion which are simply the geodesics. Assuming small velocities (i.e., $dt/d\tau \approx 1$) and weak fields the equations of motion for the rectangular components are

$$\frac{d\vec{v}}{dt} = -\frac{\vec{\nabla}V}{m}\ . \tag{9}$$

Taking the dot product of the rectangular components of the velocity, $\vec{v}$, on both sides of equation (9) and integrating

$$\frac{1}{2}mv^2 + V = \frac{p^2}{2m} + V \ = \text{constant.} \tag{10}$$

Hence, the energy, E, in equation (8) is also constant.

For small velocities and weak fields the last equation of motion is

$$\frac{d^2(ct)}{ds^2} = -\frac{2}{mc^2}\vec{\nabla}V\cdot\frac{d\vec{r}}{cd\tau} = \frac{2}{mc^2}\frac{dW}{cd\tau} \tag{11}$$

where use has been made of $ds = cd\tau$ and W is the work done on the particle. Integrating once

$$\frac{dt}{d\tau} = C + \frac{2W}{mc^2}\ . \tag{12}$$

The clock rates can be synchronized by setting $\frac{dt}{d\tau} = 1$ at $W = 0$. Then $C = 1$ and equation (12) can be written,

$$\frac{d\tau}{dt} = 1 - \frac{2W}{mc^2}\qquad . \tag{12'}$$

A similar result can be obtained from the metric in equation (1) where

$$1 = \left(1+\frac{2V}{mc^2}\right)\left(\frac{dt}{d\tau}\right)^2 - \frac{1}{c^2}\left[\left(\frac{dx}{dt}\right)^2+\left(\frac{dy}{dt}\right)^2+\left(\frac{dz}{dt}\right)^2\right]\left(\frac{dt}{d\tau}\right)^2. \tag{13}$$

This reduces to

$$\frac{d\tau}{dt} = \sqrt{1 - \frac{2}{mc^2}\left(\frac{1}{2}mv^2 - V\right)} = \sqrt{1 - \frac{2(T-V)}{mc^2}} \quad , \tag{14}$$

or

$$\frac{d\tau}{dt} = \sqrt{1 - 2\tilde{L}} \quad , \qquad \tilde{L} = \frac{L}{mc^2} \tag{15}$$

where $\tilde{L}$ is the "specific Lagrangian, and T is the kinetic energy . Note that there is an arbitrary constant in the potential energy that can be set so that $d\tau/dt=1$ when the clocks are synchronized. Equation (14) is exactly the same as equation (12'). This can be shown by noting that $dL=dT-dV$, while from equation (10) $dT = - dV=dW$. This makes $dL=2dW$ or $L=2W+C$ and equations (12`) and (15) are identical.

Equation (15) is the desired relationship. For weak fields this can be approximated as

$$\frac{d\tau}{dt} = 1 - \tilde{L} \, . \tag{15a}$$

Appendix F. Time Dilation and Work Done for a Hydrogen Atom

The Clock Principle can be used to find the changes in the clock rates if the work done is substituted into the space-time metric. Recall that the Schwarzschild metric, for small velocities and weak fields can be written as

$$c^2 d\tau^2 = \left(1 + \frac{2V}{mc^2}\right) c^2 dt^2 - dx^2 - dy^2 - dz^2 , \tag{1}$$

and that equation (1) can be written as

$$d\tau^2 = \left(1 - \frac{2L}{mc^2}\right) dt^2 , \tag{2}$$

where $L = T - V$ is the Lagrangian. The work done in the particle by all the forces is

$$W = \int \vec{F} \cdot d\vec{r} , \tag{3}$$

where $d\vec{r} = dx\vec{i} + dy\vec{j} + dz\vec{k}$. If the forces are conservative, then $\vec{F} = -\vec{\nabla} V$. Hence,

$$W = -\int \vec{\nabla} V \cdot d\vec{r} = -V . \tag{4}$$

The constant resulting from the integration can be neglected by calibrating the clocks so the rates are equal when V is zero. Using the work done the Lagrangian can now be written as

$$L = T + W . \tag{5}$$

The metric now becomes

$$d\tau^2 = \left[1 - \frac{2(T+W)}{mc^2}\right] dt^2 . \tag{6}$$

Consider the case of a hydrogen atom in an electric field. A stable configuration exists with the hydrogen atom oriented as in Figure 1. Let the proton be at

$$\vec{r}_p = x_p \vec{i} + y_p \vec{j} + z_p \vec{k} \quad , \tag{7}$$

and let the electron be at

$$\vec{r}_e = x_e \vec{i} + y_e \vec{j} + z_e \vec{k} . \tag{8}$$

The distance between them is

$$R_0 = \sqrt{(x_p - x_e)^2 + (y_p - y_e)^2 + (z_p - z_e)^2} . \tag{9}$$

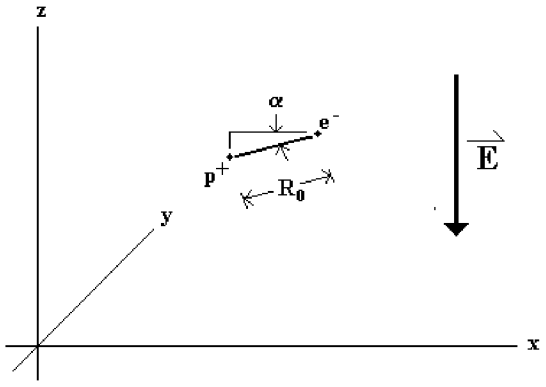

Figure 1. Hydrogen Atom in an External Electric Field

The potential energy at the location of the proton is given by

$$V = \frac{e^2}{4\pi\varepsilon_0 R_0} - eEz_p \,, \tag{10}$$

where e the magnitude of the charge on the electron, $\vec{E}$ is the electric field strength, and ε_0 is the permittivity of free space. The force on the proton is given by

$$\vec{F} = -\vec{\nabla}_p V \,, \tag{11}$$

where $\vec{\nabla}_p$ is the gradient with respect to the proton coordinates x_p, y_p, and z_p.

Then

$$\vec{F} = \frac{e^2\left[(x_p - x_e)\vec{i} + (y_p - y_e)\vec{j} + (z_p - z_e)\vec{k}\right]}{4\pi\varepsilon_0 R_0^{3/2}} + eE\vec{k} \,. \tag{12}$$

The equilibrium angle for the configuration in Figure 1 is given by

$$\sin\alpha = \frac{eE}{(e^2/4\pi\varepsilon_0 R_0^2)} = \frac{z_p - z_e}{R_0} \,. \tag{13}$$

The force now becomes

$$\vec{F} = -\frac{e^2\left[(x_p - x_e)\vec{i} + (y_p - y_e)\vec{j}\right]}{4\pi\varepsilon_0 R_0^{3/2}} \,. \tag{14}$$

In order to calculate the work done assume the projected orbits of the electron and the proton are circles in the x-y plane, then

$$\vec{r}_p = R_p\left[\vec{i}\cos(\omega t) + \vec{j}\sin(\omega t)\right] + v_0 t\vec{k} \,, \tag{15}$$

where t is the time, v_0 is the speed of the proton in the z-direction, ω is the angular velocity, and R_p is the radius of the proton's orbit given by

$$R_p = \frac{m_e}{m_p + m_e} R_0 \cos\alpha \,. \tag{16}$$

The quantities m_e and m_p are the mass of the electron and proton respectively. The force can now be written as

$$\vec{F} = \frac{e^2\left[\vec{i}\cos(\omega t) + \vec{j}\sin(\omega t)\right]}{4\pi\varepsilon_0 R_0^2} \tag{17}$$

The work done on the proton is

$$W = \int \vec{F} \cdot d\vec{r}_p = 0 \tag{18}$$

Since the kinetic energy is also constant, there will be no change in the clock rates associated with the proton.

Appendix G. Quantum Aharonov-Bohm Effect Consistent with New Theory

The spacetime metric in the Theory of General Relativity is basic to an understanding of the four dimensional motion of particles in a gravitational field. For small fields and small velocities the interval can be written as

$$d\tau^2 = (1+2\frac{\varphi}{c^2})dt^2 - \frac{1}{c^2}(dx^2+dy^2+dz^2)\,. \tag{1}$$

Where φ is the potential energy per unit mass, τ is the proper time, t is the coordinate time, x, y, z are the rectangular coordinates, and c is the speed of light. An extension of General Relativity to electromagnetic fields can be developed by considering the potential for a gravitational field due to a point mass M at the origin. For this case the potential is given by

$$\varphi = \frac{-GM}{r} = \frac{-GMm}{mr}\,. \tag{2}$$

Where $r^2 = x^2 + y^2 + z^2$ is the distance from the source mass to the particle of mass m, and G is the gravitational constant. For small electromagnetic fields and small velocities,

$$\varphi = \frac{e(-\phi + \vec{v}\cdot\vec{A})}{m}\,. \tag{3}$$

Where $\vec{v}$ is the particle velocity, ϕ is the electric potential $\vec{A}$ is the magnetic potential, and e is the charge of the particle. For the case of no electric field the interval in equation (1) becomes

$$d\tau^2 = (1+2\frac{e\vec{v}\cdot\vec{A}}{mc^3})dt^2 - \frac{1}{c^2}(dx^2+dy^2+dz^2)\,. \tag{4}$$

The relative rates of proper time and coordinate time can now be readily found for small fields and small particle velocities

$$\frac{dt}{d\tau} = 1 - \frac{e\vec{v}\cdot\vec{A}}{mc^3} + \frac{1}{2}\left(\frac{v}{c}\right)^2, \tag{5}$$

. The elapsed coordinate time between two spacetime points 1 and 2 is given in terms of the proper time by

$$t_{1-2} = \int_1^2 \left[1 - \frac{e\vec{v}\cdot\vec{A}}{mc^3} + \frac{1}{2}\left(\frac{v}{c}\right)^2\right] d\tau\,. \tag{6}$$

In the Aharonov-Bohm experiment over the two distinct paths (see Figure 1) the difference in arrival times is

$$\Delta t = t_{3-4} - t_{1-2} = \int_3^4 \left[1 - \frac{e\vec{v}\cdot\vec{A}}{mc^3} + \frac{1}{2}\left(\frac{v}{c}\right)^2\right] d\tau - \int_1^2 \left[1 - \frac{e\vec{v}\cdot\vec{A}}{mc^3} + \frac{1}{2}\left(\frac{v}{c}\right)^2\right] d\tau$$

or, $$\Delta t = \int_4^3 \left(\frac{e\vec{v}\cdot\vec{A}}{mc^3}\right) d\tau + \int_1^2 \left(\frac{e\vec{v}\cdot\vec{A}}{mc^3}\right) d\tau \tag{7}$$

Over the paths from 2-3 and 4-1 the particle is at an infinite distance from the solenoid and there is no contribution to the difference in times. Hence, we can write

$$\Delta t = \oint_C \left(\frac{e\vec{A}\cdot\vec{v}d\tau}{mc^3} \right) d\tau = \oint_C \frac{e\vec{A}\cdot d\vec{s}}{mc^3}. \tag{8}$$

Where C is the closed contour 1-2-4-3-1 in Figure 1. The quantity $\oint_C \vec{A}\cdot d\vec{s}$ is just the magnetic flux Φ contained within the contour C. Hence,

$$\Delta t = \frac{e\Phi}{mc^3} \tag{9}$$

In the Aharonov-Bohm experiment, the quantum phase angle difference, $\Delta\alpha$, is measured making equation

$$\Delta\alpha = \omega\Delta t = \frac{\omega e\Phi}{mc^3}. \tag{10}$$

Where ω is the frequency of particle in the rest frame of the particle, that is

$$\omega = \frac{mc^2}{\hbar}. \tag{11}$$

Equations (10) and (11) give for the phase difference

$$\Delta\alpha = \frac{e\Phi}{\hbar c}. \tag{12}$$

This is the correct expression for the Aharonov-Bohm experiment. Note that General Relativity is incapable of predicting the change in phase unless electromagnetic potentials are included in the metric. Hence, the Aharonov-Bohm effect is an indication that there is a geometric interpretation for electromagnetic effects.

Finally, the quantity eΦ is quantized according to

$$e\Phi = 2\pi n\hbar c \tag{13}$$

Hence, from equation (9), for a particle of mass m, time and space may be quantized according to

$$\Delta t = \frac{2\pi n\hbar}{mc^2}, \quad \Delta s = c\Delta t = \frac{2\pi n\hbar}{mc} \tag{14}$$

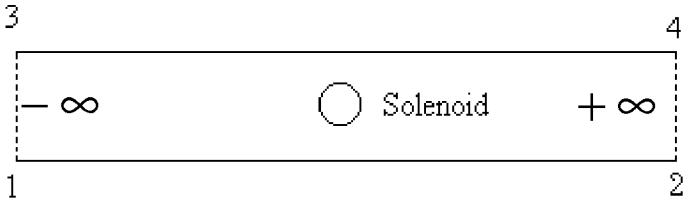

Figure 1. Two particle paths past a perfect solenoid from points 1 and 3 at - ∞ to 2 and 4 at + ∞

References

1. Harry I. Ringermacher and Brice N. Cassenti , *Search for Effects of an Electrostatic Potential on Clocks in the Frame of Reference of a Charged Particle*, Breakthrough Propulsion Physics Workshop, (NASA Lewis Research Center, Cleveland, August 12-14, 1997 , NASA publ. CP-208694 , 1999, Millis &Williamson, ed.

2. E. Schrödinger, *Space-Time Structure*, (Cambridge University Press, 1986)

3. H. I. Ringermacher, *Classical and Quantum Grav.* , **11**, 2383 (1994)

4. "Mathematica" was used to test for invariance of the Modified Einstein equations in this theory under a purely time-dependent potential in g_{00}. The solutions to the equations were found to be invariant under an additive time-dependent potential.

5. Clifford M. Will, *Was Einstein Right? Putting General Relativity to the Test,* Basic Books, Inc., Publishers, New York, 1986

6. J. Vargas, *Foundations of Physics* **21**, 379 (1991)

7. J. A. Schouten (1954), *Ricci-Calculus* , pp.126-150, (Springer-Verlag, 2nd Ed.).

8. D. Lovelock and H. Rund, *Tensors, Differential Forms, and Variational Principles* (Dover, 1989)

9. J. J. Sakurai, *Advanced Quantum Mechanics*, (Addison Wesley, 1967)

REPORT DOCUMENTATION PAGE

Form Approved
OMB No. 0704-0188

1. AGENCY USE ONLY (*Leave blank*)	2. REPORT DATE	3. REPORT TYPE AND DATES COVERED
	November 2005	Final Contractor Report

4. TITLE AND SUBTITLE

Search for Effects of an Electrostatic Potential on Clocks in the Frame of Reference of a Charged Particle

5. FUNDING NUMBERS

WBS–22–713–74–70
NAS3–00094

6. AUTHOR(S)

Harry I. Ringermacher, Mark S. Conradi, and Brice N. Cassenti

7. PERFORMING ORGANIZATION NAME(S) AND ADDRESS(ES)

KRONOTRAN Enterprises, LLC
1054 Main Street
Delanson, New York 12053

8. PERFORMING ORGANIZATION REPORT NUMBER

E–15323

9. SPONSORING/MONITORING AGENCY NAME(S) AND ADDRESS(ES)

National Aeronautics and Space Administration
Washington, DC 20546–0001

10. SPONSORING/MONITORING AGENCY REPORT NUMBER

NASA CR—2005-213999
AIAA–2001–3906

11. SUPPLEMENTARY NOTES

Prepared for the 37th Joint Propulsion Conference and Exhibit cosponsored by the AIAA, SAE, AIChE, and ASME, Salt Lake City, Utah, July 8–11, 2001. Harry I. Ringermacher, KRONOTRAN Enterprises, LLC, 1054 Main Street, Delanson, New York 12053; Mark S. Conradi, Washington University, Department of Physics, 1 Brookings Drive, St. Louis, Missouri 63130; and Brice N. Cassenti, United Technologies Research Center, 411 Silver Lane, East Hartford, Connecticut 06108. Project Manager, Marc G. Millis, Propulsion Systems Division, NASA Glenn Research Center, organization code RTP, 216–977–9535.

12a. DISTRIBUTION/AVAILABILITY STATEMENT

Unclassified - Unlimited
Subject Categories: 20 and 70

Available electronically at http://gltrs.grc.nasa.gov

This publication is available from the NASA Center for AeroSpace Information, 301–621–0390.

12b. DISTRIBUTION CODE

13. ABSTRACT ***(Maximum 200 words)***

Results of experiments to confirm a theory that links classical electromagnetism with the geometry of spacetime are described. The theory, based on the introduction of a Torsion tensor into Einstein's equations and following the approach of Schrödinger, predicts effects on clocks attached to charged particles, subject to intense electric fields, analogous to the effects on clocks in a gravitational field. We show that in order to interpret this theory, one must re-interpret all clock changes—both gravitational and electromagnetic—as arising from changes in potential energy and not merely potential. The clock is provided naturally by proton spins in hydrogen atoms subject to Nuclear Magnetic Resonance trials. No frequency change of clocks was observed to a resolution of 6310^{-9}. A new "Clock Principle" was postulated to explain the null result. There are two possible implications of the experiments: (a) The Clock Principle is invalid and, in fact, no metric theory incorporating electromagnetism is possible; (b) The Clock Principle is valid and it follows that a negative rest mass cannot exist.

14. SUBJECT TERMS

Space propulsion; Gravitation; Electric field; NMR

15. NUMBER OF PAGES

50

16. PRICE CODE

17. SECURITY CLASSIFICATION OF REPORT	18. SECURITY CLASSIFICATION OF THIS PAGE	19. SECURITY CLASSIFICATION OF ABSTRACT	20. LIMITATION OF ABSTRACT
Unclassified	Unclassified	Unclassified	